



Assessment and monitoring of land condition in the Iberian Peninsula, 1989–2000

Gabriel del Barrio ^{a,*}, Juan Puigdefabregas ^a, Maria E. Sanjuan ^a, Marion Stellmes ^b, Alberto Ruiz ^a

^a Estacion Experimental de Zonas Aridas (CSIC), Sacramento Road, 04120 La Cañada de San Urbano, Almeria, Spain

^b Remote Sensing Department, FB VI Geography/Geosciences, University of Trier, D-54286 Trier, Germany

ARTICLE INFO

Article history:

Received 17 April 2009

Received in revised form 25 January 2010

Accepted 17 March 2010

Keywords:

Desertification

Land degradation

Land condition

Assessment and monitoring

Rain use efficiency

NOAA-AVHRR

MEDOKADS

Time-series analysis

Iberian Peninsula

ABSTRACT

Diagnosis of land condition is a basic prerequisite for finding the degradation of a territory under climatic and human pressures leading to desertification. Ecosystemic approaches, such as the one presented here, address ecosystem maturity or resilience. They are low cost, not very prone to error propagation and well-suited to implementation on remotely sensed time-series data covering large areas. The purposes of this work were to develop a land condition surveillance methodology based on the amount of biomass produced per unit rainfall, and to test it on the Iberian Peninsula.

In this article, we propose parallel and complementary synchronic assessment and diachronic monitoring procedures to overcome the paradox of monitoring as a sequence of assessments. This is intrinsically contradictory when dealing with complex landscape mosaics, as relative estimators commonly produced for assessment are often difficult to set in a meaningful time sequence. Our approach is built on monthly time-series of two types of data, a vegetation density estimator (Green Vegetation Fraction-GVF) derived from Global Environmental Monitoring satellite archives, and corresponding interpolated climate fields. Rain Use Efficiency (RUE) is computed on two time scales to generate assessment classes. This enables detrended comparisons across different climate zones and provides automatic detection of reference areas to obtain relative RUE. The monitoring procedure uses raw GVF change rates over time and aridity in a stepwise regression to generate subclasses of discriminated trends for those drivers. The results of assessment and monitoring are then combined to yield the land condition diagnostics through explicit rules that associate their respective categories.

The approach was tested in the Iberian Peninsula for the period 1989 to 2000 using monthly GVF images derived from the 1-km MEDOKADS archive based on the NOAA-AVHRR sensors, and a corresponding archive of climate variables. The resulting land condition was validated against independent data from the Natura 2000 network of conservation reserves. In very general terms, land was found to be healthier than expected, with localised spots of ongoing degradation that were associated with current or recent intensive land use. Static or positive vegetation growth rates were detected almost everywhere, including Mediterranean areas that had undergone increased aridification during the study period. Interestingly, degrading or static trends prevailed in degraded or unusually degraded land, whereas trends to improve were most represented in land in good or unusually good condition.

© 2010 Elsevier Inc. All rights reserved.

1. Introduction

The land degradation concept aims at covering a range of climate and human-induced processes leading to a decline in soil potential to sustain plant productivity. The first attempt to produce a global assessment occurred at the end of the last century, resulting in the Global Assessment of Soil Degradation (GLASOD) (Oldeman et al., 1991). GLASOD was a qualitative assessment, largely based on expert judgement that distinguished the main processes leading to soil degradation, such as water and wind erosion–sedimentation, soil and water salinisation, loss of soil organic carbon and nutrients, loss of soil

structure, etc. The GLASOD database was used in the preparation of the World Atlas of Desertification (UNEP, 1992).

Later on, the GLASOD approach was upgraded in a new worldwide project entitled Land Degradation Assessment in Drylands (LADA, 2006) sponsored by the United Nations Environment Program, the Global Environmental Facility and the Food and Agricultural Organization. Whilst retaining the original GLASOD soil degradation categories, LADA took a step forward by aiming at quantitative deliverables. This was achieved by including socio-economic drivers and by enlarging its scope to carbon balance and biodiversity as components of the functional land system and its degradation.

A third global initiative with implications for land degradation assessment was the Millennium Ecosystem Assessment (MA) developed from 2001 through 2005. Its desertification synthesis (Adeel et al., 2005) evaluates the status of desertification in drylands by

* Corresponding author.

E-mail address: gabriel@eeza.csic.es (G. del Barrio).

asking key questions and providing answers based exclusively on the reports generated for the MA. It yields a consistent picture of links between land degradation, global change and biodiversity loss. It also includes guidelines for improving assessment and monitoring approaches by accounting for the role of human action and climate variability.

The three aforementioned projects reveal a historical trend of increasing complexity in approaches to land degradation assessment, which go from considering effects on 'soil' to explicitly including drivers on 'land', to being more concerned with global interaction of desertification with the atmospheric system through changes in land surface properties, and wide-scale effects on downstream delivery of water and sediments due to changes in hillslope to channel connectivity. This trend has largely been propelled by the United Nations Convention to Combat Desertification (UNCCD) 1994 definition of desertification as 'The land degradation in arid and semi-arid and dry-sub-humid areas resulting from various factors, including climatic variations and human activities'. This definition, in spite of its generality and simplicity, has the advantage of providing a benchmark for designing assessment and diagnostic methods. The outcome or symptom of desertification is land degradation, and its driving forces are climate variation and human activities. Furthermore, land degradation is defined by the UNCCD as 'the loss of land's biological and economic productivity and complexity'. This is a holistic definition that focuses on the overall impact rather than on particular causes like soil erosion, salinisation, etc.

Whilst retaining that holistic character of the land degradation concept, we propose an ecosystemic approach evolved from the original UNCCD definition, in which, land condition becomes the key to interaction between biophysical and human systems in the desertification process. There are several ecosystem attributes that can be associated with ecosystem maturity or complexity. In this context, a landscape's long-term capacity to retain, utilise and recycle local resources, and to buffer environmental changes, provides an objective basis for assessing its ecological functionality or condition.

Procedures based on this approach are relatively unsophisticated. They provide process-based indices that work by measuring the deviation in land condition status between any particular location and a reference one. They therefore demand few data, are low cost, not very prone to error propagation and well-suited to implementation on remotely sensed time-series data for application to large areas. One of such procedures is described here.

The main purpose of this project was to develop a land condition diagnostics methodology for large territories during a given time period. The target user profile was specified as a national or international institution building an information support system for a national desertification plan, or the UNCCD. The requirements were the following: i) an operational definition of land condition to be based on ecologically interpretable functions; ii) input data from already existing, generally available sources; iii) objective and repeatable procedures, leading to consistent results, even if found by different teams; and iv) results connecting explicit technical elements of land condition with lay understanding of desertification. The Iberian Peninsula was an ideal benchmark for this kind of approach because it combines a suite of land degradation syndromes that spread over wide climate gradients. Therefore, a second purpose was to apply and validate the proposed diagnostic method in that territory.

The Compact Oxford English Dictionary (Soanes & Stevenson, 2005) defines assessment as "evaluation or estimation", and monitoring as "to keep under observation, especially as to regulate, record or control". It is a common assumption in environmental science that monitoring can be built on assessments repeated over time. However, this is true only if the boundary conditions under which assessments are made remain constant. Climate is a boundary condition for land degradation. A changing climate may lead to different assessments

even if land condition remains constant. In this work, the term assessment therefore refers to the synchronic estimation of land condition made over a relatively long time period, and the term monitoring refers to the diachronic observation of vegetation trends during the same period. This period should be long enough to collect a representative sample of vegetation performance. The combination of assessment and monitoring results is thus expected to yield meaningful land condition diagnostics.

2. Data

2.1. Study area, period and resolutions

The Iberian Peninsula is occupied by Portugal and Spain and extends over ca. 581,000 km² (Fig. 1). It is a rugged country criss-crossed by mountain ranges, many of their divides exceeding 2000 m.a.s.l. Enclosed by them, two large central plateaus and some tectonic basins define the main drainage network, which includes several rivers over 500 km long. Synoptic air masses create a NW to SE precipitation gradient, ranging from Atlantic humid climate zones on the north and west coasts, to pure Mediterranean on the east coast, the SE corner becoming the most arid zone of Europe. Indicative total annual precipitation in those extremes is 1600 and 140 mm/year, respectively. In addition, altitudinal temperature and precipitation gradients are associated with the main mountain ranges, creating a genuinely alpine climate in the Pyrenees, and well distributed extra-zonal belts of humidity elsewhere.

The Iberian Peninsula has a mosaic of land cover that includes significant areas of traditional and newly developed agriculture (49% of land), embedded in a matrix of natural and semi-natural vegetation (47% of land) (EEA, 2007). The former includes most of the present-day active desertification hot spots, whilst somewhat stabilized areas of inherited desertification associated with historical processes since the 15th century are well represented in the latter (Puigdefabregas & Mendizabal, 1998).

The period of analysis was intended to reflect a fair range of mid-term vegetation performance. Two practical conditions were formulated for its selection: i) only complete years to be used because the methodology is partly based on yearly summaries; and ii) only complete fields within the period (*i.e.* no gaps to be filled using statistical techniques) to meet both the applied and the methodological goals. Continuity of the time-series input was not strictly required as long as some yearly sequences were included and eventual gaps were grouped discretely in between. Years were defined in a manner similar to the meteorological convention reflecting the progression of hydrological and ecological seasons. Hydrological years encompass whole annual pulses that include the season of maximum soil moisture recharge and conclude with the season of maximum evapotranspiration (Glickman, 2000). Summer is relatively dry in most of the Iberian Peninsula, and first precipitations after the warm period usually fall in September. That reason is why the definition used for hydrological year throughout this study is from 1 September to 31 August.

The period of analysis was set as September 1989 through August 2000 to maximize the continuity of a vegetation and climate input data time-series whilst containing full hydrological years. A failure of the National Oceanic and Atmospheric Administration-Advanced Very High Resolution Radiometer (NOAA-AVHRR) at the end of 1994 and consequently missing input data for the derivation of Green Vegetation Fraction estimates resulted in a gap from August 1994 to January 1995 in the Green Vegetation Fraction time-series (see the next section). Because hydrological years are from September to August, data from both 1993–94 and 1994–95 had to be excluded. Therefore the number of whole years available for calculation was limited to 9. The climatic representativeness of these years is discussed below in the description of the climate archive. Nevertheless,

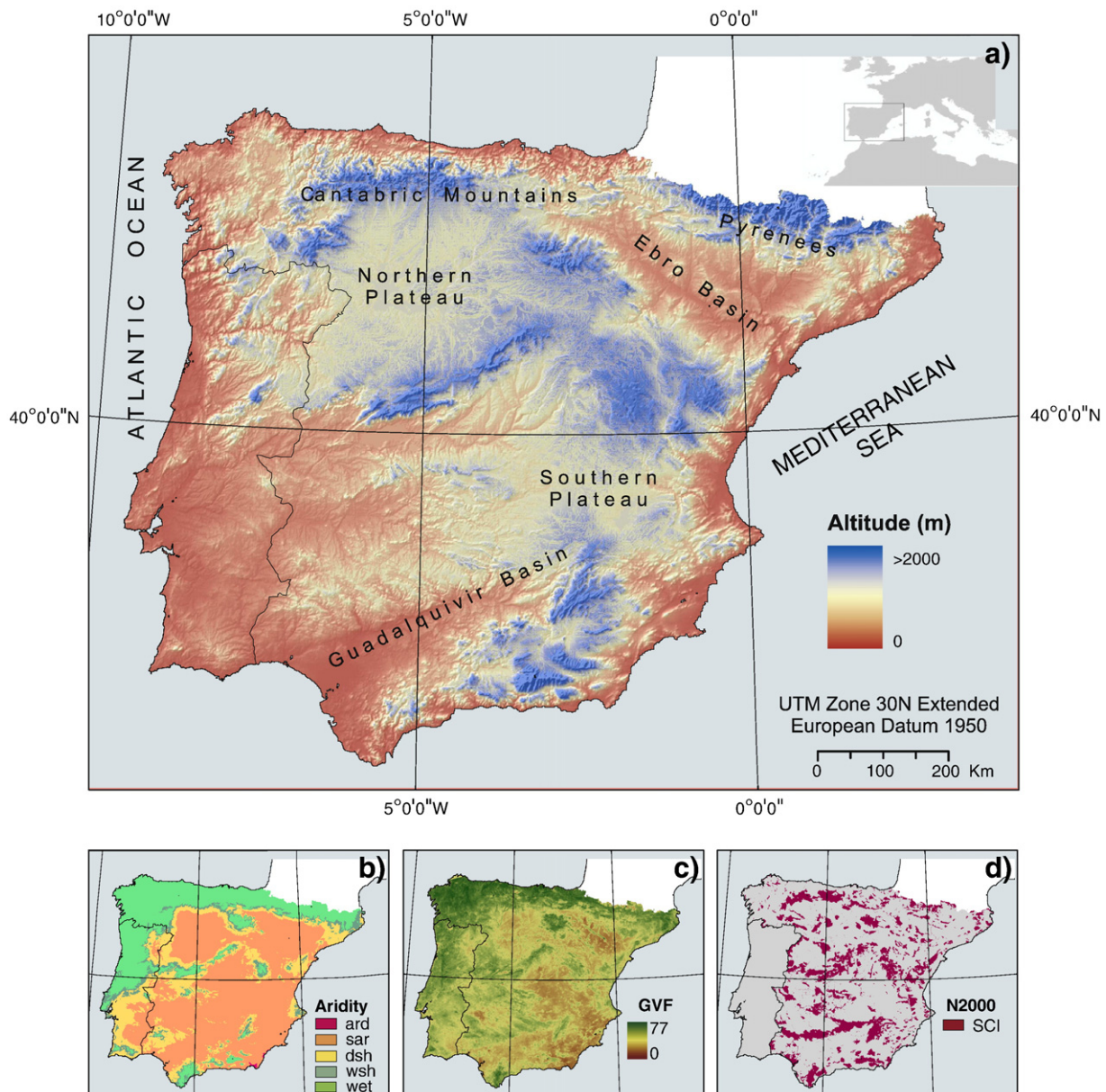


Fig. 1. Location and main geographic features of the Iberian Peninsula. *a)* Dominant relief patterns. *b)* Mean annual aridity, 1970–2000. UNEP classes are shown: arid (ARD), semi-arid (SAR), dry subhumid (DSH), wet subhumid (WSH), and wet (WET). *c)* Mean monthly vegetation density, 1989–2000. Green Vegetation Fraction shown is for a reference range of 1 to 100. *d)* Natura 2000 network in continental Spain (N2000), showing the distribution of Sites of Community Interest (SCI).

that period immediately follows the accession of Portugal and Spain to the European Economic Community in 1986, and their ratification of the Treaty of the European Union in 1992. The important changes required in both countries for their adaptation were reflected in their respective landscapes and therefore make a suitable framework for this study. The spatial and temporal resolutions necessary to capture those changes were 1000 m and 1 month respectively.

2.2. Green vegetation fraction

The approach presented needs a consistent and reliable time-series archive of a proxy for net primary productivity, such as vegetation surrogates from remote sensing data. Satellite data files with coarse geometric, but high temporal resolution, have been successfully employed for monitoring vegetation at a regional to global scale (Goetz et al., 2006; Tucker & Nicholson, 1999). Due to their high repetition rate these data provide better geographical coverage and temporal monitoring at the expense of spatial detail. At

present, NOAA-AVHRR sensors provide the most comprehensive time-series of satellite measured surrogates for regional-scale surface conditions. The Normalized Difference Vegetation Index (NDVI) which is derived from the reflectance bands in the red and near infrared domain is a commonly accepted surrogate for vegetation cover, volume and vitality (e.g. Hielkema et al., 1987; Myneni et al., 1997; Tucker, 1979).

However, the NDVI is known to be influenced by soil and rock background (Price, 1993). Furthermore, it is sensitive to parameters such as atmospheric conditions due to aerosol properties and concentration and gaseous components, illumination, and the observation geometry, although this is supposedly partly eliminated by temporal maximum-value compositing of the data (Holben, 1986). Moreover, NDVI values are platform-dependant due to different spectral properties as well as the observation geometry, which complicates direct comparison of different sensors. The time-series archive used in this study is based on an unmixing approach making use of the well-known relationship of vegetation cover and surface

temperature (T_s) and overcomes some of the limitations of the NDVI. It is based on the observation that under dry conditions the land surface temperature is inversely proportional to the amount of vegetation canopy cover and thus, the NDVI. This is due to a variety of factors including latent heat transfer through evapotranspiration, lower heat capacity and thermal inertia of vegetation compared to soil (Choudhury, 1989; Goward & Hope, 1989). Whilst on a small spatial scale the variation in vegetation species and soil classes may show high variability (Choudhury, 1989), a coarse geometric resolution shows the variation in surface temperature to be mainly caused by the vegetation fraction (Nemani et al., 1993). As there are local gradients related to altitude and exposure, temperature variation due to soil moisture, variable evaporation and evapotranspiration respectively, and remaining cloud artefacts (e.g. Lambin & Ehrlich, 1996; Sandholt et al., 2002), the feature space covers a triangle or trapezoid. This feature space, amongst others, has been used for deriving parameters like soil moisture content (e.g. Chuvieco et al., 2004; Nemani et al., 1993; Sandholt et al., 2002) and improving land cover classification (Lambin & Ehrlich, 1997). The linear unmixing approach derives Green Vegetation Fraction (GVF) from the triangle described above. The three vertices were derived and served as endmembers (full vegetation cover, dry soil and the 'cold' endmember representing the wet edge of the triangle) to unmix the feature space, thereby deriving GVF estimates (Stellmes et al., 2005; Weissteiner et al., 2008). The relationship between NDVI and T_s as described above develops only under stable atmospheric conditions, which are often present in semi-arid to arid areas, especially from spring to autumn. This approach, if such conditions were not given, would cause a bias in the estimated GVF. This constraint was accounted for by labeling data which did not fulfill the prerequisite as 'no data'. A detailed description of the technical implementation of the NDVI- T_s unmixing approach and derivation of GVF can be found in Stellmes et al. (2005) and Weissteiner et al. (2008).

The NOAA AVHRR Archive used to derive the GVF is the "Mediterranean Extended Daily One Km AVHRR Data Set" (MEDOKADS) processed and distributed by the Free University of Berlin (Koslowsky, 1996). The MEDOKADS archive, which covers the period from 1989 to 2005 and is delivered as 10-day composites, comprises full resolution AVHRR channel data, NDVI, T_s and additional auxiliary data with a geometric resolution of about 1 km². This includes correction for sensor degradation and orbital drift effects that cause non-linear changes in the signal measured, as well as inter-calibration between the AVHRR/2 (NOAA 11 and NOAA 14) and AVHRR/3 (NOAA 16) sensors to prevent inhomogeneities in the time-series. A detailed description of data pre-processing may be found in Koslowsky (1996, 1998) and Friedrich and Koslowsky (2009). T_s is derived by the split window approach (Coll & Caselles, 1997; Coll et al., 1994) and normalized to the time of the local sun zenith plus 1 h and 42 min (Billing, 2007).

2.3. Climate archive

The climate time-series was extracted from an archive of monthly fields of mean maximum, mean and mean minimum air temperatures, and of total precipitation, generated for 1970–2000 for the Iberian Peninsula. This archive was interpolated from monthly summaries of georeferenced meteorological stations throughout the territory. Data for Portugal were downloaded from the Portuguese Water Resources Information System (<http://snirh.pt>, accessed January 2010) and complemented with series from AgriBase (Instituto Superior de Agronomia). Data for Spain were received from the Spanish State Agency of Meteorology. Gaps in the data fields were not filled in using statistical techniques. Station monthly summaries were computed only for stations with less than 5 days of missing data for the corresponding month, and interpolation for any given month was done using only stations with complete monthly summaries for the corresponding year. This resulted in variable networks of input

stations for each surface, averaging 390 and 1877 points for temperature and precipitation surfaces respectively. In addition to these, approximately 10% of stations were reserved to enable cross-validation of the resulting surface.

Interpolation was done using thin-plate smoothing as implemented in ANUSPLIN (Hutchinson, 1995), an accepted technique to interpolate noisy multivariate data such as climatic variables, which has performed well in comparisons with other spatial interpolation methods (Hutchinson & Gessler, 1994; Jarvis & Stuart, 2001; Price et al., 2000). Latitude, longitude and altitude were specified as covariates for surface fitting. Temperature data were input raw, but precipitation was transformed to its square root during the interpolation to reduce skewness. The finest resolution of the thin plate smoothing surfaces was 3 arc-min, which was then registered to a 1000 m grid.

ANUSPLIN generates internal statistics that can be used to assess the quality of any fitted surface. The Square Root of the Mean Square Error (RTMSE) is a true estimator of the overall interpolation error. It is an absolute error in the same units as the original variable, but its ratio to the mean produces a relative error that is related to the predictive error of the interpolated surface. The degrees of freedom of the fitted surface are estimated through the signal. This parameter ranges from zero to the number of data points. Extremes are interpreted as failed spatial optimisation, from either under or overfitting, whilst around half the number of data points are considered appropriate (Price et al., 2000). Smooth transitions of signal from one month to the next are an indicator of the absence of systematic errors.

The signal to data point ratio was below 50% for temperature surfaces, with many values between 25% and 35%. This suggests limitations in the number of input data points which may have resulted in a loss of detail on the interpolated surfaces. This is not necessarily bad in terms of broad spatial patterns, but it does indicate that absolute predictions should be used with caution for fine microclimatic patterns. Mean maximum temperature signals are higher in summer, and mean minimum temperatures in winter, suggesting that the corresponding surfaces have at least partially succeeded in reflecting the complex patterns associated with the main relief mesoforms of the Iberian Peninsula. For precipitation, the signal to data point ratio was around 50%, which can be considered appropriate, although again, slightly on the low side because the admissible range only extends to 80% for this variable. Both temperature and precipitation series show uniform signals, which we interpret as a combination of the regional influences of climate. Smooth signal transitions between months reflect absence of bias.

The RTMSE was lower than 1 °C for all temperatures. The highest error in the mean maximum temperatures was 0.85 °C in the peak summer months, and mean minimum temperatures tended to concentrate the highest errors up to 0.73 °C in late summer and autumn. This probably adds to the previous interpretation concerning excessive smoothing of the respective surfaces. Absolute errors in precipitation did range from 4.41 mm in July to 12.82 mm in December, but the seasonal pattern of prediction errors was inverse and corresponded to 24% and 13% respectively.

Those results can be compared to others using the same interpolation technique. Yan et al. (2005) found RTMSEs of 0.42 to 0.83 °C for temperature surfaces, and 2 to 15 mm for precipitation surfaces interpolated for China, the latter with predictive errors ranging from 8 to 15%. And the findings of McKenney et al. (2006), working on Canada and United States, in general less than 1.5 °C for temperature, and 20 to 40% for precipitation, were also comparable.

Precipitation is a critical factor in this study, and the climate archive described above can provide some insight on the representativeness of the hydrological years in the 1989–2000 study period compared to the 1970–2000 reference period. The reference mean annual precipitation for the whole Iberian Peninsula is 705 mm. Compared to this, the driest years in the study period were 1998–99 (–28%), 1994–95 (–22%) and 1992–93 (–16%). The wettest years

were 1995–96 (+28%), 1996–97 (+19%) and 1997–98 (+18%). These figures are only indicative, but in addition to the temporal variability they suggest, wide spatial variation is also associated with geographic gradients in this large, complex study area. This can be checked using individual maps of standardised residuals that show how much each location departs from its own mean during the reference period in any given year (Fig. 2). Two important conclusions may be drawn from those maps. First, a year that is not especially anomalous when precipitation is averaged over the whole area can still contain extreme deviations for individual locations. This occurred in 1989–90, which although it was only 7% wetter overall, still shows wide contrasts between locations that received much more or much less precipitation than their respective local average. And second, local extreme deviations do not necessarily occur in the overall driest years. For example, the driest year in a zone in the Northern Plateau was 1991–92 with precipitation of approximately 2.3 standard deviations below the local mean, and this is well below the precipitations received in 1998–99 and 1994–95, which were -1.2 and -0.6 standard deviations respectively.

The methodology applied in this work relies on the detection of vegetation performance under spatial and temporal ranges of climatic conditions. From this point of view, the main requirement for input data is the availability of a wide spectrum of variability in local precipitation rather than over the whole study area. The 9 years used in this work encompass a fair representation of such variability given the elements discussed in the preceding paragraph. Whilst it obviously would have been preferable to include 1993–94 and 1994–95, these years do not contain unique or extreme features that would prevent safe application of this approach.

2.4. Other complementary data

Three additional data sets were used in this work. The Global 30 Arc-Second Elevation Dataset (GTOPO30) (EROS, 1996) was used as an indirect source of topographic data for generation of the GVF and the climate archives. COoRdinate INformation on the Environment (CORINE) is a programme managed by the European Environment Agency (EEA, 2007) to provide consistent information on land cover and land cover changes in Europe at a spatial scale of 1:100,000 with a decadal temporal resolution. The editions for the reference years 1990 (abbreviated CLC1990) and 2000 (abbreviated CLC2000) were used in the selection of input data and as an external control to assist in interpreting the results. Finally, the subset for continental Spain (MARM, 2006) of the Natura 2000 network, established in 1992 (EEC, 1992) to provide a coherent structure for nature protection areas across the European Union, was used for validating the results. These data sets are described as necessary in the corresponding sections below.

3. Methods

The diagnostic procedure involves independent assessment and monitoring components that operate on the same database. On the one hand, the assessment component aims at quantifying the relative performance of each landscape location with respect to its reference potential conditions. Therefore, each cell is synchronically compared to all others over the period of analysis. On the other hand, the monitoring component aims at detecting evolution of every location over time, both because of its response to changing climate drivers

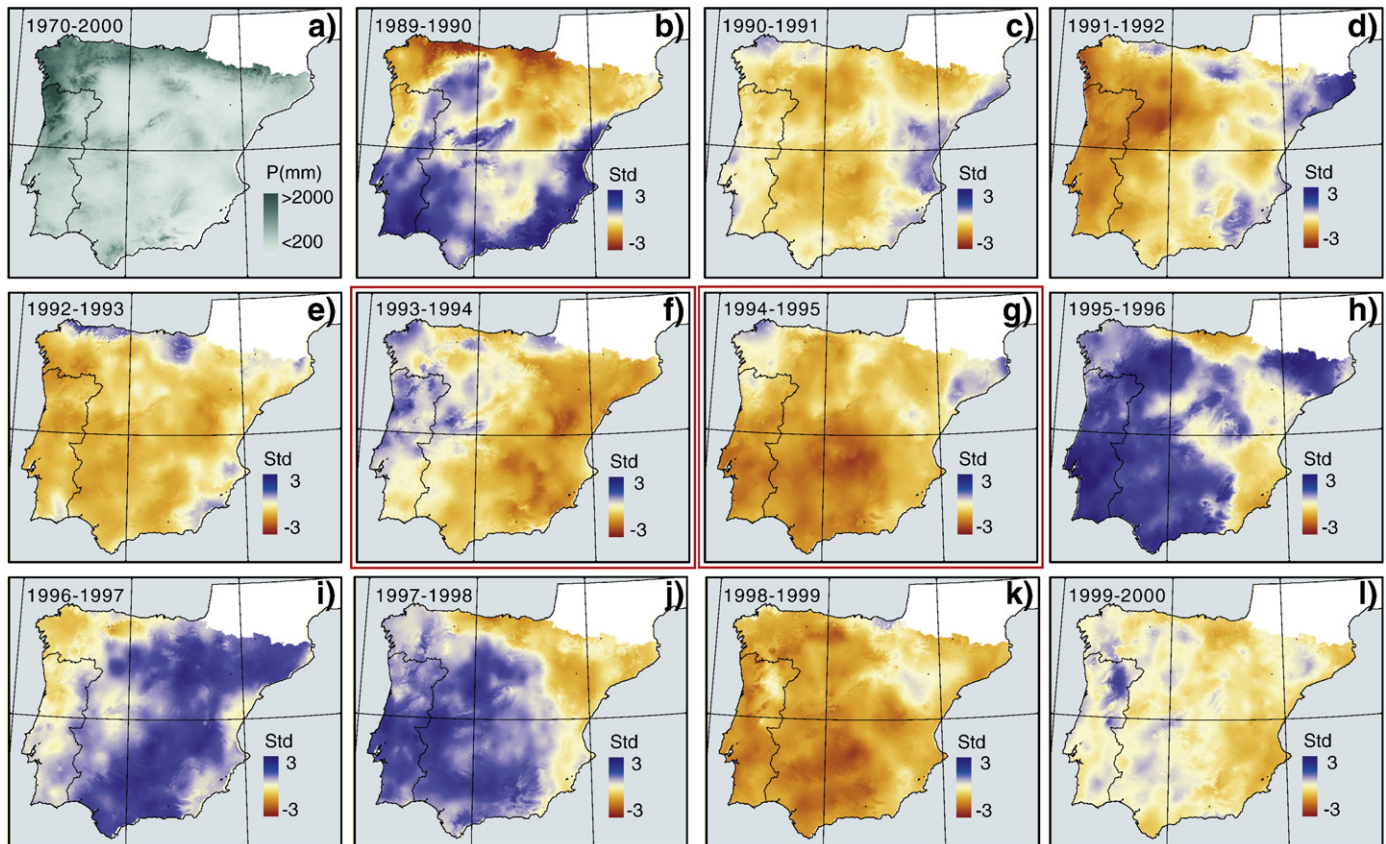


Fig. 2. Representativeness of the period of analysis (1989–2000) in the precipitation reference period (1970–2000) for the Iberian Peninsula. Hydrological years are shown. a) Mean annual precipitation in the reference period. b) through l) Yearly departures from the local reference mean in standard deviation units. Years 1993–1994 and 1994–1995 were excluded from the analysis and are highlighted in red.

and because of its internal ecological dynamics, so each cell is diachronically compared to itself over the same period. The results of assessment and monitoring then converge in the land condition diagnostics component through explicit rules that associate their respective categories.

The methods described in this article have been coded in R and are available in a software package called *r2dRue* which can be downloaded from any Comprehensive R Archive Network (CRAN) mirror at <http://www.r-project.org/> (accessed January 2010).

3.1. Assessment

The reduction of plant biomass and Net Primary Productivity (NPP) below those of land not desertified under equivalent environmental conditions is proportional to land degradation undergone. This is an accepted perception of land condition and the most closely related to the UNCCD definition of desertification. Both biomass and NPP can be reasonably estimated using satellite-derived information (Tucker et al., 1986). Two ecosystem attributes are relevant for this assessment, annual average biomass and seasonal or inter-annual growth peaks. The first shows the ecosystem's long-term capacity to sustain biomass, whilst the second concerns its resilience for recovering from disturbances, in particular, rainfall fluctuation (Pickup, 1996). Annual average biomass and NPP may be expected to decrease along land degradation gradients whilst peak NPP (resilience) is at its maximum at intermediate degradation states (Pickup et al., 1994).

Rain Use Efficiency (RUE) was originally defined as the ratio of NPP to precipitation (P) over a given time period (LeHouerou, 1984), in which may be interpreted as proportional to the fraction of P released to the atmosphere through the vegetation cover. This ratio is a suitable descriptor of ecosystem condition because it can only be higher if the soil remains fully functional, and in this context it has been used to describe the sustainable carrying capacity in rangelands (Guevara et al., 1996). The NDVI has been used before as a suitable NPP proxy in the computation of RUE using satellite imagery as input data (Prince et al., 1998). Similarly, an appropriate integration over time of the Green Vegetation Fraction (GVF) described in the preceding section was used here as a surrogate NPP.

The formulation of RUE as a ratio implies that it can be expected to be higher for drier conditions if vegetation remains constant. If the RUE is computed over a large area with strong climatic gradients, as it is the case of the Iberian Peninsula, drylands often account for the highest values because of their very low P, which impedes direct comparison between locations under different climates. To avoid this, RUEs were plotted against an Aridity Index (AI) that was computed for the corresponding period as the ratio of potential evapotranspiration (PET) to P. This formulation is as simple as that of UNEP (1992), but the inverted terms expand the numerical scale of drylands without resorting to too many decimals, and also make it slightly more intuitive. The method of Hargreaves and Samani (1982) was used to compute PET using temperatures from the climate archive and extra-terrestrial solar radiation.

Only areas of rainfed natural and seminatural vegetation were used for the RUE vs. AI scatterplot, thereby ensuring that only climate driving forces were considered. A selection mask was therefore constructed to extract all the locations that maintain the same land cover allocation in CLC1990 and in CLC2000, and belong to one of the following categories: coniferous forest, mixed forest, natural grassland, moors and heathland, sclerophyllous vegetation, transitional woodland-shrub, beaches, dunes and sand plains, bare rock, sparsely vegetated areas, burnt areas, and glaciers and perpetual snow.

The upper and lower boundaries of this scatterplot are interpreted to convey the maximal and minimal vegetation performance, respectively, for a given aridity, which is a first step in detrending climate. These boundaries were computed by first identifying 10 classes of AI in the scatterplot using regular percentiles of the AI frequency distribution

over the study area, then extracting the 95th (for the upper boundary) and 5th (for the lower boundary) percentiles of RUE for each of these classes, and finally, empirically fitting a function to each of the series of 10 RUE percentile and AI class median pairs. The boundary functions were selected by optimising statistical significance whilst maintaining the model as simple as possible under visual inspection. The resulting functions could then be spatially modelled using the AI layer as the independent variable, yielding two layers showing the expected maximum and minimum RUE, respectively, for every map location. Similar rescaling was done by Boer and Puigdefabregas (2003) for potential vegetation index prediction, and by Wessels et al. (2008) for generating relative NPP on a land capability gradient.

A relative RUE (rRUE) was then computed to yield a new layer showing the position of the RUE observed in each location within the range of its maximum and minimum potential. Values of rRUE should therefore range from 0 to 1, and it is assumed to reflect vegetation condition in terms of observed performance with respect to the minimum and maximum performances found empirically for that climate. Because these boundaries were derived from percentiles, and because they correspond to natural vegetation, some locations were expected to exceed that range. This was useful for detecting zonal anomalies. For example, the relatively large plant biomass in irrigated areas receiving water from topographical or technical sources not accounted for by this method, was properly detected as 'overperforming' (i.e. rRUE greater than 1) when processed by the procedure described.

The rRUE has two important properties. First, because the RUE boundary functions were fitted from RUE percentiles within each AI class, the expected maximum and minimum RUE for each location was already corrected for the local AI, and therefore the rRUE map was climatically detrended. And second, the RUE boundary functions are a natural benchmark for potential vegetation performance for a given aridity, against which any location can be compared whatever its land cover. In this sense the rRUE map was also detrended with respect to land uses under the assumption that undisturbed natural vegetation shows optimum performance in terms of RUE. This means that direct comparisons could be made between any two locations irrespective of their dominant climate or land use.

The detailed operation of the RUE concept used in this approach has been omitted from the above description for the sake of simplicity. Beyond that, the definition of the period over which observed RUE is computed targets different responses of the vegetation cover. Long-term RUE computed over full years may reflect average biomass and can be compared to ecological maturity in the framework of the ecosystemic approach described in the Introduction. However, short-term RUE computed using only antecedent precipitation would rather reflect immediate response capacity and can be interpreted in terms of productivity or resilience. This is why two implementations were used here. In the first one, an overall mean observed RUE (RUE_{OBS_me}) was computed for the full period ($n = 9$ years) by averaging annual observed RUE. Each of these was computed over a hydrological year as the mean of 12 monthly GVFs divided by the sum of 12 P. For month i in year j :

$$RUE_{OBS_me} = \frac{1}{n} \cdot \sum_{j=1}^n \left(\frac{\frac{1}{12} \cdot \left(\sum_{i=1}^{12} GVF_{j,i} \right)}{\sum_{i=1}^{12} P_{j,i}} \right). \quad (1)$$

The corresponding overall mean aridity index (AI_{OBS_me}) is computed accordingly:

$$AI_{OBS_me} = \frac{1}{n} \cdot \sum_{j=1}^n \left(\frac{\sum_{i=1}^{12} PET_{j,i}}{\sum_{i=1}^{12} P_{j,i}} \right). \quad (2)$$

In the second implementation, an extreme observed RUE (RUE_{OBS_ex}) was computed again for the full period. In this case, the maximum GVF in each cell (GVF_t) was selected from among the monthly data available in the time-series, and this was then divided by the sum of P over the six months preceding the month (t) when that maximum was detected. The result was a composite layer, as the maximum GVF appeared in each cell at a different time:

$$RUE_{OBS_ex} = \frac{GVF_t}{\sum_{i=1}^6 P_{t-i}} \quad (3)$$

An associated aridity index (AI_{OBS_ex}) was also computed for this particular six month period:

$$AI_{OBS_ex} = \frac{\sum_{i=1}^6 PET_{t-i}}{\sum_{i=1}^6 P_{t-i}} \quad (4)$$

Both implementations of observed RUE (RUE_{OBS_me} and RUE_{OBS_ex}) were processed following the steps described above to find their respective boundary functions and relative values ($rRUE_{me}$ and $rRUE_{ex}$ respectively; computation is shown for the first):

$$rRUE_{me} = \frac{RUE_{OBS_me} - RUE_{EXP_me_P05}}{RUE_{EXP_me_P95} - RUE_{EXP_me_P05}} \quad (5)$$

where the subscripts $_{P05}$ and $_{P95}$ refer respectively to the expected minimum and maximum RUE corresponding to the aridity in each location, given by the boundary functions (subscript $_{EXP}$) as explained above in the scatterplot procedure.

The distinction between mean and extreme RUE is considered potentially useful, as they may be different for vegetation types depending on the type of cover (e.g. annual plants, irrigated areas, forests, etc.).

The use of the mean of 12 monthly GVFs to compute annual observed RUE (Eq. 1) departs from the convention of approaching NPP through a summatory of individual values of the selected vegetation index. It was done this way to facilitate frequent follow-up of the process by querying input and output layers in search of spatial and seasonal errors, as all of them would share the order of magnitude. This consideration also applies to the monitoring component of our approach (see the following Section). The division by a constant term of 12 has no effect on the relative spatial or temporal variations in cumulative GVF, as it is computed anyway. The study by Bai et al. (2005), which can be taken as an example of experimental confirmation of this, reports two relevant findings. They compared NDVI-based indicators of land degradation derived from the Global Inventory Modelling and Mapping Studies (GIMMS) dataset, both between them and with RUE estimates. On one hand, they found a very high correlation ($r^2 = 1$) between the mean and sum of NDVI values, and also similar temporal trends, and were therefore considered alternates. On the other, highly significant correlations ($p < 0.001$) were detected between RUE estimates computed using NPP data derived from a carbon exchange model and those derived from the NDVI, again considering them alternates. In our assessment component, computation of relative RUE from the boundary functions (Eq. 5) further transforms the numerical scale of observed RUE into a common reference range of 0 to 1, whatever the scale of the original estimate.

3.2. Monitoring

Changes in plant biomass over time make an accepted indicator of trends in land condition. A gradual depletion of biomass is generally

interpreted as ongoing degradation, and reciprocally, an increase is interpreted as improvement in a responsive ecosystem. It is important to remark that such a basic understanding refers only to rates of change, and is therefore independent of the bulk ecosystem biomass, which was an issue in the assessment explained above.

In this case, RUE could not be used to monitor vegetation trends during the period for two reasons: the bias associated with the use of precipitation both as for the computation of RUE and as a tested predictor (Hein & de Ridder, 2006), and the relative nature of detrending in the computation of rRUE. Raw GVF was therefore used instead.

When using low resolution Earth Observation in a large territory, trends in plant biomass can be simplified as driven by two factors: climate and internal ecological dynamics. Only the second is relevant to land condition, as it can be related to a secondary succession. Therefore, monitoring of plant biomass along relatively long periods requires accounting for possible effects of a drifting climate. Failing to do so might result, for example, in erroneously interpreting a piece of healthy land as degrading, when biomass is declining simply because of decreasing precipitation.

Multiple stepwise regression was carried out to isolate the effects of time and climate on the green biomass in each cell. As resolution was yearly, each cell entered a regression with 9 points. In each of these, the dependent variable was the yearly mean of 12 monthly GVF values, and the two predictors were the year sequence number and the yearly AI computed using the corresponding 12 months. The purpose of this analysis was to detect partial contributions of the two predictors, creating significant trends in the dependent variable (not to make predictions of the latter for given values of the former). Accordingly, the regressions were used in a standardised form, in which the partial regression coefficients are expressed in standard deviation units, rather than in the original units of each variable (such coefficients are also known as beta coefficients). This enabled direct comparison of the relative strength of time and aridity for imprinting a change of one standard deviation on the GVF. All the procedures followed the formulations in Sokal and Rohlf (1995).

When there is a correlation between the two predictors, as might be the case with time and aridity, the overall significance of a multiple regression may not be indicative of their individual effects. Hence, a second independent variable must be incorporated in the regression model only as long as the additional increment of determination it produces is significant. We proceeded to deal with this requirement in the following way. First, the coefficient of multiple determination was computed using both time and aridity as predictors ($R^2_{GVF_{1,2}}$), and its overall significance was tested to a threshold of $\alpha = 0.10$. For significant cases, the second variable in the multiple regression was the one with the lowest simple correlation coefficient with GVF (r_{GVF_2}). Then the increment in the determination due to the second variable over the determination using the first variable alone was tested by comparing the observed statistic F_s :

$$F_s = \frac{R^2_{GVF_{1,2}} - r^2_{GVF_2}}{(1 - R^2_{GVF_{1,2}}) / (n - 3)} \quad (6)$$

with the expected F -distribution at a threshold of $\alpha = 0.10$ for 1 and $n - 3$ degrees of freedom ($F_{\alpha = 0.10[1, n-3]}$), where n is the number of data points. Eq. (6) shows a simplified formulation of this step using only two independent variables. The parameters used are commonly provided by statistical software packages and are not described here.

If this was also significant, a multiple regression would be accepted and the respective standard partial regression coefficients would be used to quantify the effects of both time and aridity. Otherwise, simple regressions were explored for each variable through the significance of its respective correlation coefficient. For significance at $\alpha = 0.10$,

the corresponding correlation coefficient was used as a standard single regression coefficient because it is by definition the slope of a regression in standard deviation units. If no significance was found in any of the above tests, GVF was assumed not to be affected by either time or aridity.

3.3. Land condition

The assessment and monitoring tasks described in the sections above aimed at yielding four basic maps quantitatively reflecting four different land condition components, overall relative biomass (in terms of $rRUE_{me}$), overall relative productivity (in terms of $rRUE_{ex}$), biomass response to aridity and biomass response to time (in terms of their respective standard partial or simple regression coefficients) as primary products to be used as elementary information in land management or additional modelling. Further to that, a higher level understanding of land condition in the study area was gained by simplifying their respective individual information to binary attributes, which were subsequently combined to produce the legend categories on the land condition map.

In the assessment task, both implementations of relative RUE were ranked and defined in turn by boundary functions associated with percentiles. Hence, by definition, there will always be locations outside these ranks. A broad summary of land performance in reaching and maintaining an optimal biomass was therefore achieved by classifying each of the relative RUEs into three basic categories: below range (lower than 0), within range (0 to 1), and above range (greater than 1).

The obvious criterion for reclassifying monitoring results was whether biomass had a positive, negative, or non significant trend over time or aridity.

Each of the four basic maps was thus reclassified into three categories. Hence a merely combinatorial approach could yield up to 81 classes of land condition. That undesirable complexity was overcome in a meaningful manner by composing the legend on the final map on two hierarchical levels. The higher one corresponded to assessment classes and indicated the state of land, whilst the lower level was found using monitoring attributes to indicate land trends over time. The final definition of this legend depends somewhat upon the final results and required some adaptation in consistency with the concept of degradation. Therefore, legend classes and subclasses are precisely described in Section 4 of this article.

3.4. Validation

Land condition is a rather abstract concept that was applied in this work on a decadal time span. This, and the relatively coarse spatial resolution, prevented directly testing the results against field observations. In practical terms, the validation of an approach like the one presented here should meet two basic conditions, the spatial scale of validation data should be comparable to that of the final land condition map, and the information conveyed by this validation dataset should be interpretable at a level of abstraction equivalent to that of the land condition concept.

For validation, we employed a set of spatially distributed data for which a landscape condition could be assumed, the Natura 2000 network Sites of Community Interest (SCI). This European conservation network was set up in 1992, and SCI land condition can be taken as representative of the study period. The SCI network in continental Spain includes 853 designated sites, which accounts for 22% of the territory (Fig. 1d). Because their designation aimed at representing relevant natural species and habitats, it contains a variety of landscapes. And because the conservation of those habitats is the network's main purpose, conditions in the portion of territory included in it can be assumed to be favourable for vegetation to thrive. The Natura 2000 network includes natural and semi-natural landscapes where

traditional management is allowed, but land uses leading to the over-exploitation of natural resources are normally excluded. Whilst traditional management does not necessarily mean sustainable management, in general terms, land condition within the Natura 2000 space can be expected to be good, and our validation is based on this working hypothesis.

Validation was done using mainland Spain (about 85% of the Iberian Peninsula) as the test area, at a working resolution of 1 km. The concrete purpose was to find out whether there is an association between landscape conservation, in terms of membership in the Natura 2000 network, and land condition, in terms of the final output map classes. A sample of 45,731 cells, roughly representing 10% of the whole test area, was extracted from the original maps using a stratified-random design. This dataset was assumed to be made up of independent samples, including absence of spatial autocorrelation.

A chi-square test was done for the null hypothesis that there is no association between conservation status and land condition. The sample dataset described above was divided in two groups defined by membership to Natura 2000, and the proportions of cases belonging to the land condition classes were compared. The test evaluates whether or not the differences observed in these proportions significantly exceed those that could be expected by mere chance (Siegel & Castellan, 1988). To do this, an observed statistic (χ^2) was computed from the sample data and its probability was then found in the chi-square distribution. If the alternative hypothesis was accepted, the residual (*i.e.* observed minus expected) frequencies would be used to interpret the sense and meaning of that association.

It could be argued that the use of conservation reserves to validate land condition is incomplete because only better condition classes are tested. This is only partly true. In fact, these classes are expected to be around the upper boundary of observed RUE over aridity. It is therefore this boundary that is really validated, that is, the maximum reference condition against which all the locations of a given degree of aridity will be assessed.

4. Results

4.1. Assessment

Scatterplots and boundary functions of observed RUE over aridity are shown in Fig. 3a and b. In the absence of a theoretical criterion for a particular model for those functions, several models were tested and the most significant fit was selected in each case (Table 1). It is worthy of note that the increase in mean observed RUE becomes gentler with increasing aridity, which is confirmed by the inverse model selected for both boundary functions. On the contrary, extreme observed RUE increases with aridity confined within an upper power and a lower quadratic boundary function.

The resulting relative RUE maps are shown in Fig. 3c and d. The distribution of values does not reflect any apparent climatic bias in either map. Patches with high mean relative RUE are scattered around the study area, some of them associated with the banks of major rivers. Extreme relative RUE is somewhat spotty because it is a composite map. In spite of this, zones with high values are consistently detected surrounding the Ebro basin and in the Northern Plateau.

As expected, the geographic patterns of mean and extreme relative RUE do not generally match. This is clearer in the contingency table shown in Table 2. The dominant combination is by far the one with both estimators of relative RUE within the 0 to 1 range. This is a predictable outcome of the method, as the respective boundary functions were fitted to percentiles that enclose the majority of the data points. That middle combination should be taken as a baseline condition where acceptable oscillation is associated with land management and cover.

Whenever any of the relative RUE estimators exceeds the stated range, it should generally be interpreted as a deviation associated

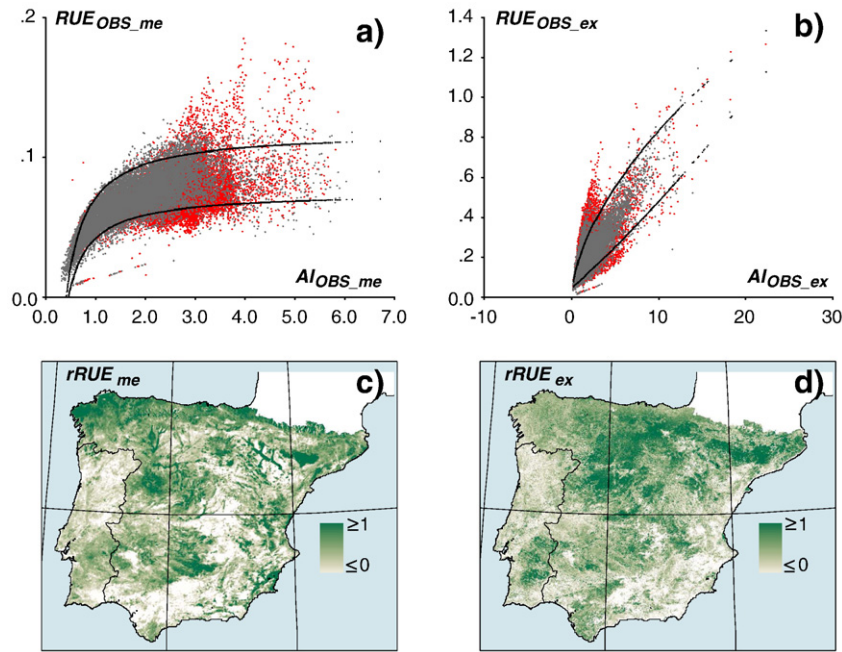


Fig. 3. Rain Use Efficiency (RUE) in the Iberian Peninsula (1989–2000), computed as the inter-annual mean of each location over the full period (a and c), and for the six-month period preceding the time when maximum vegetation density was detected at each location (b and d). Empirical boundary functions fitted to the scatterplots of observed RUE over aridity (a: RUE_{OBS_me} vs. AI_{OBS_me} ; b: RUE_{OBS_ex} vs. AI_{OBS_ex}) define the potential limits of expected RUE for any aridity level. Only locations of rainfed natural and seminatural vegetation (grey dots) were used to fit the boundaries, whilst irrigated crops and other surfaces not responding to climate (red dots) are shown for information. Relative RUE (c: $rRUE_{me}$; d: $rRUE_{ex}$) is then computed for each location as the position of its observed RUE within the referred limits.

with under or overperforming vegetation in the respective component. Apart from the baseline combination, mean and extreme relative RUEs assess land condition similarly in 3.41% of the locations. However, the sum of combinations where both estimators differ in their results accounts for 24.19% of the study area, which suggests that they convey different information. In two of these combinations, mean and extreme relative RUE yield completely opposite results. They represent 0.18% of the study area and are considered as uninterpretable anomalies.

The assessment map legend (Fig. 4) was made using the combinations in Table 2 as follows. Locations where the mean and extreme relative RUE are below range were considered to be consistently underperforming in terms of the basic interpretation of RUE, and were reclassified to unusually degraded land. If one of the estimators was below range whilst the other was within range, the corresponding locations were reclassified to degraded land. The baseline combination where both mean and extreme relative RUE were within range was considered to represent land in good condition. And any other combination where either of the estimators was above range (except the two anomalies) was considered to be overperforming and was therefore reclassified as land in unusually good condition.

4.2. Monitoring

The significance of effects of time and aridity on the GVF is shown in Fig. 5a. Approximately 5% of the Iberian Peninsula showed a

significant response to both time and aridity in the regression procedure. This is comparatively low with respect to the proportion of individual responses to any single predictor (40%), and is likely to be associated with the fact that a stepwise approach is more conservative than a simultaneous multiple one. 55% of the study area did not show any linear response to either of the predictors.

Fig. 5b and c shows the effect of aridity and of time, respectively, on GVF over the study period. Correlation coefficients and standard partial regression coefficients have been combined on the same map for each of the predictors depending on whether a significant single or multiple regression was fitted at every location. They are mere reclassifications by the coefficients sign, however they are useful in displaying the geographic distribution of effects. Aridity produces large patches of negative effects (i.e. depletion of GVF with increasing aridity) which are well distributed over the areas of Mediterranean influence, whilst positive effects are confined to northern mountain ranges such as the Pyrenees and Cantabric mountains. The effect of time on GVF is positive in the vast majority of locations where a significant relationship was detected, and only a few small spots scattered over the Mediterranean area show GVF depletion over time.

The monitoring map was then made by using significance categories (Fig. 5a) as a mask, and the sign of effects (Fig. 5b and c) to identify trends. Its legend includes all the possible combinations of single or multiple and positive or negative effects, and is further detailed in Table 3. In general, effects of aridity should be attributed to climatic variation within the study period, and effects of time to the overall trend

Table 1

Parameters of the boundary functions fitted to the 5th and 95th percentiles of observed RUE vs. aridity. $RUE_{EXP_me_p05}$: mean expected RUE at 5th percentile; $RUE_{EXP_me_p95}$: mean expected RUE at 95th percentile; $RUE_{EXP_ex_p05}$: extreme expected RUE at 5th percentile; $RUE_{EXP_ex_p95}$: extreme expected RUE at 95th percentile; AI_{OBS_me} : observed mean aridity index; AI_{OBS_ex} : observed aridity index computed for the six-month period preceding the month when maximum vegetation density was detected.

Y	X	Model	b_0	b_1	b_2	p
$RUE_{EXP_me_p05}$	AI_{OBS_me}	$Y = b_0 + (b_1/X)$	0.076	-0.033		<10E-4
$RUE_{EXP_me_p95}$	AI_{OBS_me}	$Y = b_0 + (b_1/X)$	0.119	-0.047		<10E-4
$RUE_{EXP_ex_p05}$	AI_{OBS_ex}	$Y = b_0 + b_1 \cdot X + b_2 \cdot X^2$	0.047	0.040	4E-4	<10E-4
$RUE_{EXP_ex_p95}$	AI_{OBS_ex}	$Y = b_0 \cdot X^{b_1}$	0.218	0.584		<10E-4

Table 2
Contingency table of mean vs. extreme relative RUE ($rRUE_{me}$ and $rRUE_{ex}$ respectively) after their classification in three basic intervals. Table entries are: assessment class allocation and total area [km^2 (%)].

	$rRUE_{me} < 0$	$0 \leq rRUE_{me} \leq 1$	$1 < rRUE_{me}$	Total
$rRUE_{ex} < 0$	Unus. Degr. 14,261 (2.45)	Degr. 24,914 (4.28)	Anomaly 340 (0.06)	39,515 (6.79)
$0 \leq rRUE_{ex} \leq 1$	Degr. 391,47 (6.73)	Good 421,094 (72.40)	Unus. Good 28,612 (4.92)	488,853 (84.05)
$1 < rRUE_{ex}$	Anomaly 688 (0.12)	Unus. Good 47,004 (8.08)	Unus. Good 5566 (0.96)	53,258 (9.16)
Total	54,096 (9.30)	493,012 (84.76)	34,518 (5.93)	581,626 (100.00)

of GVF excluding climatic responses. This, in turn, is associated with land management or with intrinsic ecological processes occurring in the vegetation cover. Single effects interpretation is straightforward. Both explanations are still true for multiple effects, but their importance as drivers must be in the order of the local standard partial regression coefficient strength. Table 3 reports averages, but some general interpretations are possible. For example, where GVF increases in time and decreases with aridity, the mean of the latter coefficient is stronger. It follows that arid spells or a sustained increase in aridity over the whole study period have played a dominant role in GVF depletion, but this is still accumulating over time, albeit at a slow positive rate. This is the only case in Table 3 where the mean of an aridity coefficient is higher than its equivalent time coefficient.

4.3. Land condition

The assessment map reflects bulk GVF whilst the monitoring map conveys rates of change in GVF. Land condition categories were

therefore derived from a hierarchical combination of assessment classes and monitoring subclasses. In this exercise, subclass labels were adapted to the contents of the main classes in the following ways:

- Land with no significant trends in either time or aridity was called *static* whatever its condition.
- Land with negative trends over time was called *degrading* whatever its condition.
- Land with no trends over time but with a significant response to aridity in any sense was considered to react to variation in climate. It was called *fluctuating* if the condition was degraded, and *resilient* if condition was good.
- Land with positive trends in time was called *recovering* if it was degraded, and *improving* if it was already in good condition.

Table 4 shows the details and extent of the classes and subclasses so defined, and the corresponding land condition map is shown in Fig. 6. It is important to stress that such names and definitions aim

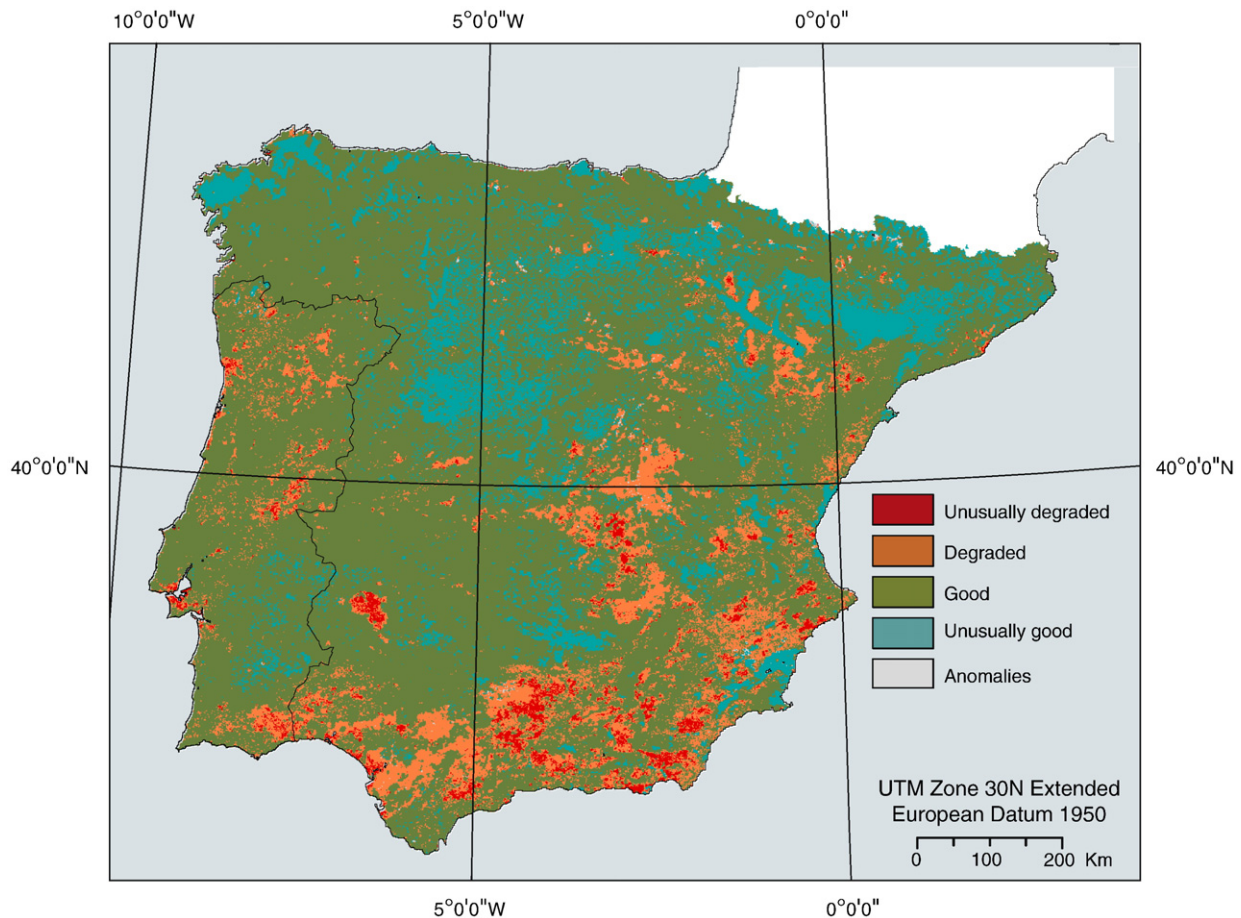


Fig. 4. Assessment of land condition in the Iberian Peninsula (1989–2000). Legend is consistent with Table 2.

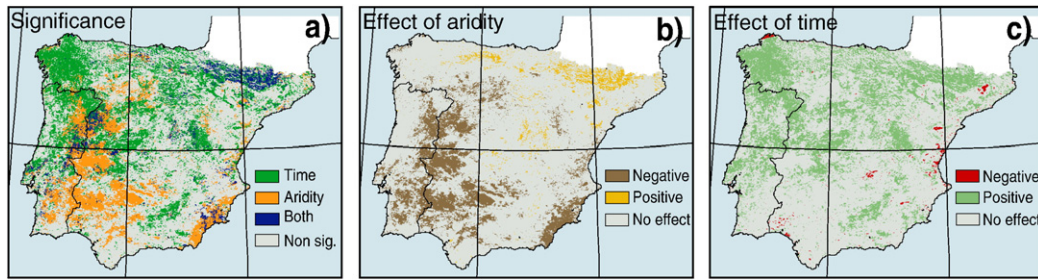


Fig. 5. Linear effects of time and aridity on Green Vegetation Fraction in the Iberian Peninsula (1989–2000). a) Significance at the threshold of $\alpha = 0.1$. Response to both predictors refers to the coefficient of multiple determination and to the increment of determination associated with the second predictor. Response to a single predictor refers to the coefficient of correlation. b) Effect of aridity in terms of the sign of the standard partial or single regression coefficient. c) Effect of time in terms of the sign of the standard partial or single regression coefficient.

only at using a consistent nomenclature at a level sufficiently generalized to deal with a large territory like the Iberian Peninsula. Hence the land condition map should be taken as a kind of broad stratification, and real diagnostics of particular locations should be made using the numerical values in the assessment and monitoring procedures.

Nevertheless, some conclusions can be drawn at that general level. First, the amount of land in any condition that is degrading is relatively small and accounts for only 0.85% of the Iberian Peninsula. This degrading trend is relatively more frequent in already degraded land, although it is still marginal even in that class. Truly static land showing no trend during the period is absolutely dominant whatever the condition (54.67% of the area), but its relative importance in assessment classes increases as condition deteriorates. It amounts to 75% of unusually degraded land, but to only 55% of land in unusually good condition. A contrary pattern is detected in land with a positive trend in time as its relative importance increases as condition improves, from unusually degraded land where recovering trends account for 12% of extension, to land in unusually good condition, where 33% of the locations are improving. On a whole, positive trends in time are detected in 29.13% of the territory. Fluctuating or resilient trends have a maximum share in intermediate condition classes, where they reach 17% of degraded land and 16% of land in good condition respectively.

The spatial distribution of the land condition categories follows some apparent geographic patterns too. Land in good condition with clearly identifiable resilient or improving patches prevails south of the Pyrenees and in the western third of Iberia, whilst static patches form a matrix in the rest of the territory in which other categories are embedded. Unusually degraded, or degraded, static land is frequent in continental areas with Mediterranean influence and in the south,

whilst fluctuating trends can be found in a large compact zone in the southeast. Finally, static and resilient land in unusually good condition are found on both central plateaus and in the northeast, whilst improving patches can be seen tracing the banks of large rivers (notably the Ebro in the northeast) and in a more compact area in the northwest corner of the Peninsula.

4.4. Validation

The chi-square test has two requirements if any of the variables has more than 2 classes: less than 20% of expected frequencies lower than 5, and no expected frequency lower than 1. As reported in the preceding Section, the land condition categories *Unusually degraded – Degrading*, and *Degraded – Degrading* are comparatively small and their further subdivision by conservation status would not meet the latter requirement. Therefore, and for validation purposes only, they were grouped with the *static* trend in their respective assessment class. Table 5 shows the results of the chi-square test of the regrouped land condition categories and conservation status. The test was significant, and therefore the alternative hypothesis that there is an association between them could be accepted. Residuals express the difference between observed and expected counts when there is no relationship between variables. Their interpretation enables further details to be inferred on the meaning of that association.

Unusually degraded, or degraded land, are negatively associated with SCI (*i.e.* classes underrepresented in conservation reserves) whatever the trends. Land in good, or unusually good condition, is also negatively associated if it is degrading. On the contrary, SCI are positively associated with land in good condition for most of the remaining trend subclasses. SCI are also positively associated with static land in unusually good condition. These basic facts are consistent with

Table 3

Relative strength of effects of time (*t*) and aridity (*AI*) on GVF (rate of change in standard deviations of GVF per one standard deviation of each predictor). Combinations correspond to areas of significant effects shown in Fig. 5. Table entries are mean and 95% confidence interval of either coefficient of correlation (*r*) for single effects, or standard partial regression coefficient (*b'*) for multiple effects; and area [km^2 (%)].

Effect of time	Effect of aridity			Total
	–	0	+	
–	<i>Degrading</i> $b'_t = -0.628 \pm 0.013$ $b'_{AI} = -0.597 \pm 0.013$ 415 (0.07)	<i>Degrading</i> $r_t = -0.716 \pm 0.003$ n.a. 4397 (0.76)	<i>Degrading</i> $b'_t = -0.817 \pm 0.025$ $b'_{AI} = 0.500 \pm 0.028$ 201 (0.03)	5013 (0.86)
0	<i>Fluct. or Resilient</i> n.a. $r_{AI} = -0.700 \pm 0.001$ 82,139 (14.12)	<i>Static</i> n.a. 318,553 (54.77)	<i>Fluct. or Resilient</i> n.a. $r_{AI} = 0.667 \pm 0.002$ 6256 (1.08)	406,948 (69.97)
+	<i>Recover. or Improving</i> $b'_t = 0.633 \pm 0.003$ $b'_{AI} = -0.670 \pm 0.004$ 14,447 (2.48)	<i>Recover. or Improving</i> $r_t = 0.721 \pm 0.000$ n.a. 140,971 (24.24)	<i>Recover. or Improving</i> $b'_t = 0.837 \pm 0.003$ $b'_{AI} = 0.562 \pm 0.002$ 14,247 (2.45)	169,665 (29.17)
Total	97,001 (16.68)	463,921 (79.76)	20,704 (3.56)	581,626

Table 4
Land condition categories in terms of the assessment and monitoring estimators. Area in the Iberian Peninsula (1989–2000) for each class and subclass.

Assessment	Monitoring		Land condition	Area [km ² (%)]
	Effect of time	Effect of aridity		
$rRUE_{me} < 0$ AND $rRUE_{ex} < 0$	–	–/0/+	Unusually degraded	14261 (2.45)
	0	0	Degrading	119 (0.02)
	0	–/+	Static	10651 (1.83)
	+	–/0/+	Fluctuating	1717 (0.30)
			Recovering	1774 (0.31)
$(rRUE_{me} < 0$ AND $0 \leq rRUE_{ex} \leq 1$ OR $0 \leq rRUE_{me} \leq 1$ AND $rRUE_{ex} < 0$)	–	–/0/+	Degraded	64061 (11.01)
	0	0	Degrading	832 (0.14)
	0	–/+	Static	42336 (7.28)
	+	–/0/+	Fluctuating	10910 (1.88)
			Recovering	9983 (1.72)
$0 \leq rRUE_{me} \leq 1$ AND $0 \leq rRUE_{ex} \leq 1$	–	–/0/+	Good	421094 (72.40)
	0	0	Degrading	3211 (0.55)
	0	–/+	Static	220019 (37.83)
	+	–/0/+	Resilient	66627 (11.46)
			Improving	131237 (22.56)
$(1 < rRUE_{me}$ AND $0 \leq rRUE_{ex} \leq 1$ OR $0 \leq rRUE_{me} \leq 1$ AND $1 < rRUE_{ex}$ OR $(1 < rRUE_{me}$ AND $1 < rRUE_{ex})$	–	–/0/+	Unusually good	81182 (13.96)
	0	0	Degrading	841 (0.14)
	0	–/+	Static	44953 (7.73)
	+	–/0/+	Resilient	8969 (1.54)
			Improving	26419 (4.54)
$(rRUE_{me} < 0$ AND $1 < rRUE_{ex})$ OR $(1 < rRUE_{me}$ AND $rRUE_{ex} < 0)$			Anomaly	1028 (0.18)
				1028 (0.18)

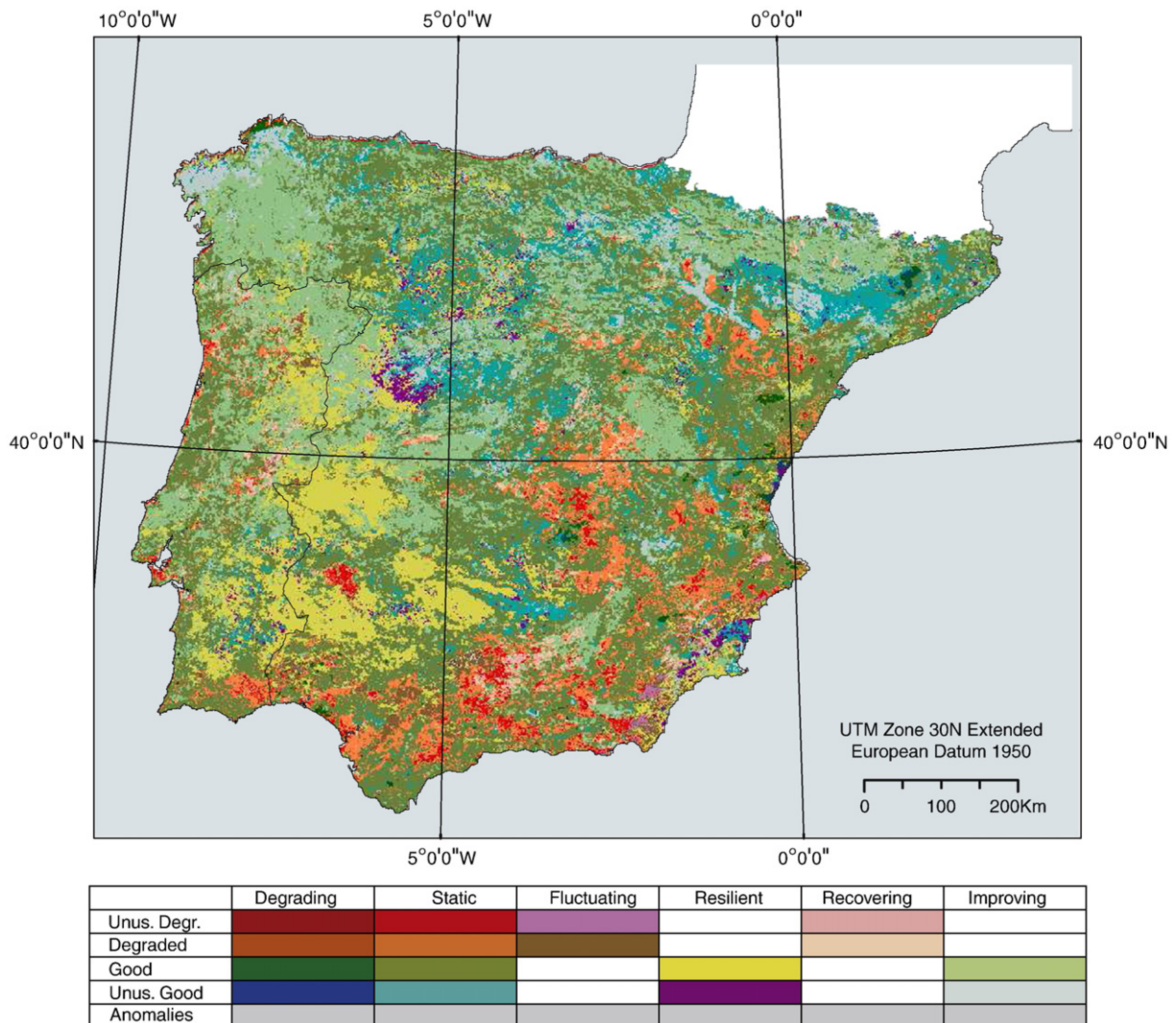


Fig. 6. Land condition map for the Iberian Peninsula (1989–2000). Legend is consistent with Table 4.

Table 5

Results of a chi-square test of regrouped land condition categories and membership to the Natura 2000 network Sites of Community Interest (SCI) in continental Spain. Table entries are residual (observed minus expected) counts ($\chi^2 = 427$, $df: 13$, $n = 45731$, $p < 10E-4$). See explanation in the text.

Land condition		Conservation status		Total
		Non-SCI	SCI	
Unusually degraded	Degrading or Static	45	−45	710
	Fluctuating	20	−20	127
	Recovering	11	−11	140
Degraded	Degrading or Static	252	−252	3558
	Fluctuating	112	−112	847
	Recovering	28	−28	622
Good Condition	Degrading	8	−8	233
	Static	−392	392	17,599
	Resilient	89	−89	4713
	Improving	−304	304	9892
Unusually good condition	Degrading	14	−14	66
	Static	−39	39	4065
	Resilient	56	56	734
	Improving	101	−101	2425
Total		35,810	9921	45,731

the conservation goals of the Natura 2000 network and back the initial working hypothesis that landscapes belonging to it are in favourable condition for maintenance and succession of the vegetation cover.

Land in unusually good condition that is improving, and resilient good condition land, are negatively associated with SCI in apparent contradiction to the general results. However, a query on the land cover of these locations did show that uses are mainly agricultural uses, often with intensive irrigation as discussed below. Therefore this exception actually confirms the type of association between conservation status and land condition and, indirectly, contributes to the validation of the latter.

5. Discussion

The section above reports on the main findings derived from the analysis performed, and interpretation is restricted to a minimum. However, there are several points in both the [Methods and Results](#) that require further discussion to better understand the results of our work.

The core of the assessment procedure is the fit of boundary functions to the scatterplot of observed RUE vs. observed aridity. The fact that a least squares model could be fitted with a high level of significance suggests that the scatterplot is compact and its shape can be approached using simple equations. This in turn supports the idea that reference areas could be statistically detected along the full gradient of aridity in the study area.

Both mean (RUE_{OBS_me}) and extreme (RUE_{OBS_ex}) observed RUE increase quickly with aridity from low values corresponding to humid locations. That is the predictable behaviour that makes RUE unsuitable for assessing vegetation cover in large regions containing different climates. Such increase tapers with aridity in the case of RUE_{OBS_me} , showing that less precipitation is compensated in the long-term by a proportional loss of density in the vegetation cover. This is at least true for the range of arid zones in the Iberian Peninsula, but it should not be extrapolated outside that range.

In contrast, extreme observed RUE increases indefinitely with aridity at a rather constant rate. Whilst that pattern is clearly observed, its explanation exceeds the scope of this work and refers to a variety of processes related to the response of vegetation to rainfall events. It has especially intriguing relationships with the findings reported by [Huxman et al. \(2004\)](#), by which very different biomes show similar and maximum RUE under water-limiting conditions. Notwithstanding, the use of a common six-month, antecedent period for all locations is an

oversimplification, and the refinement of models to detect a significant number of time lags, for example as incorporated in [Udelhoven et al. \(2009\)](#) would probably improve this, but at the expense of computation simplicity.

Nevertheless, the empirical model presented here seems to have overcome two main limitations of assessment approaches, values for zones with different climates are comparable, and reference areas can be found ([Prince et al., 2007](#); [Veron et al., 2006](#)). The second issue has been successfully approached by identifying natural reserves ([Garbulsky & Paruelo, 2004](#)), but it is difficult to maintain a strict control of climate variability and there is also a subjective component. We have done this statistically by specifying percentiles for calculating expected RUE. The Iberian Peninsula contains landscapes covering the full range of land condition in every climate zone. Therefore, the 5th and 95th percentiles were used to allow a wide symmetrical range of relative RUE results to be included in the middle assessment class. But these percentiles could be changed depending on the purpose or the characteristics of the study area, which could require some preliminary work. For example, if an area is known to be generally degraded and reference vegetation is scarce or lacking, an asymmetrical interval of percentiles in the upper ranges of observed RUE (say 40% and 95%) could still yield an unbiased assessment of land condition.

The observed RUE found within the specified percentiles define land in good condition and the reason for aiming at as wide an interval as possible is to obtain enough numerical resolution in the computation of relative RUE. Obviously, that step controls the number of locations that are considered out of range. In our study, the classes 'unusually degraded' and 'degraded' together are equivalent to 'unusually good' in terms of their definitions with respect to the range defined by 'good'. 'Good' accounts for 72.40% of the locations ([Table 2](#)), and the marginal classes together account for 27.42% almost evenly divided between below and above (the remaining 0.18% corresponds to uninterpreted anomalies). This proportion is slightly higher than the 10% that might be expected strictly from the percentiles, and the difference should be attributed to the fit of the boundary functions. In spite of that built-in concentration of observations in a middle range, the use of two observed RUE implementations leads to a meaningful discrimination of types of landscapes, as discussed below.

The stepwise multiple regression applied in the monitoring procedure proved to be useful to separate the effects of time and aridity on the GVF change rates. The climate in the Iberian Peninsula did not remain constant during the second half of the 20th century but was subject to both spatial and temporal variability ([de Luis et al., 2008](#); [Gonzalez-Hidalgo et al., 2008](#)), with an overall trend to aridification in the Mediterranean zone ([Gonzalez-Hidalgo et al., 2001](#)). Our correlation analysis (between GVF, aridity and time) was consistent with those results and showed that such climate drift was not homogeneous. Most of the Iberian Peninsula did not show significant trends, but important areas in the northwest did evolve towards greater wetness, whilst most of the Mediterranean zone experienced increased aridity.

The effects of aridity on vegetation density are known to be negative, and have been reported for large areas of the Ebro Valley in NE Spain for an equivalent period ([Vicente-Serrano et al., 2006](#)). Interestingly, [Fig. 5b](#) shows negative effects of aridity on GVF in coincident Mediterranean areas, and [Table 3](#) reveals that the magnitudes of such effects are comparable to those of time. It follows that areas where aridity and time have respectively negative and positive effects on GVF, could be misclassified as static if only time were used as a predictor. In fact, a cross tabulation between the effects of time as in [Fig. 5c](#) and an equivalent map of effects constructed using straight-forward significant correlation coefficients between time and GVF detected such a situation in 10,941 km², most of them in Mediterranean areas. A better interpretation for those areas would be that a decrease in rainfall has had a negative effect on the rates of

growth of vegetation, and once this effect is removed, it is observed to still be accumulating over time.

Increased aridity shows positive GVF effects in certain areas (Fig. 5b), mainly associated with northern mountain ranges such as the Cantabric or the Pyrenees Mountains. This occurs in wet or wet sub-humid zones and is likely to be more associated with higher temperatures in environments where this factor is limiting than to a decrease in precipitation (Vicente-Serrano et al., 2004).

Isolating the effects of aridity on vegetation trends is more than a mere methodological refinement. Rainfall anomalies cause vegetation anomalies, which allow detection of overall greening at a global level (Hellden & Tottrup, 2008). But land degradation addresses precisely what is left after such effects have been removed (Herrmann et al., 2005). It is generally accepted that a depletion of biomass is an indicator of land degradation. This has been confirmed by several studies (e.g. Geerken & Ilaiwi, 2004; Herrmann et al., 2005; Lambin & Ehrlich, 1997). Several of these studies have also taken climatic conditions directly or indirectly into account. Other studies (Olsson et al., 2005; Wessels et al., 2007) have reported on the influence of variability in precipitation on biomass directly in the Sahel zone and in southern Africa, respectively. Thus, Mulligan et al. (2004) stated that climate variability “is king” in semi-arid to arid environments and may thus camouflage human-induced changes. The stepwise regression approach implemented in this study makes it possible to assess the magnitude of the influence of the two factors, climate and time, separately. As the time factor is connected to human-induced changes, overestimation of degradation trends can be prevented.

Some additional interpretation is required to identify the types of landscapes that may be associated with the classes and subclasses on the final land condition map. We employed Level 3 of the CORINE Land Cover 2000 database (CLC2000) for two reasons, it is a comprehensive and hierarchical classification of prevailing land cover classes in Europe, and it is updated regularly, therefore enabling future repetitions of this work either in other countries or in the Iberian Peninsula.

We found a significant association between dominant CLC2000 classes and land condition categories using the same sampling network that was used for validation ($\chi^2 = 14,548$, $df=208$, $n = 45731$, $p < 10E-4$). Its complete interpretation is beyond the scope of this work, but some key relationships provide useful insights into the approach used here. For example permanently irrigated land and, to a lesser extent, fruit trees, are strongly associated with land in unusually good condition, both static and improving. Such land uses are based on water brought in from outside the system to increase vegetation density beyond the zonal standards of aridity. Therefore when such exuberant cover is evaluated relative to its local rainfall, as in RUE, it scores as overgrown. That is further accentuated by the fact that irrigation often involves intensive management to maximize production in semi-arid zones. Irrigated land then goes beyond the 95% percentile of observed RUE for its degree of aridity, and is appropriately considered as unusually good by the assessment procedure. This also explains the poor affinity between this land condition category and membership to the Natura 2000 network.

In a less extreme situation, there is a high frequency of agro-forestry and natural grasslands in resilient land in good condition, and of broad-leaved forest, coniferous forest and transitional woodland-shrubs on improving land in good condition. This mirrors the landscape in mountain ranges and abandonment of much cultivated land after Spain and Portugal joined the European Union. This trend has been reported using NOAA-AVHRR time-series data for both NE Spain (Lasanta & Vicente-Serrano, 2006; Vicente-Serrano et al., 2003) and for the whole Iberian Peninsula, where a rural exodus syndrome was identified (Hill et al., 2008). Those locations are commonly located close to the upper boundary function in our analysis.

Sparsely vegetated areas show avoidance for land in good or unusually good condition except if it is degrading, and has a high affinity for all categories of degraded or unusually degraded land. This land cover is the bottom line in all cases and is around the lower boundary function.

Areas truly limited in their vegetation performance by inherent properties of their habitat would be relatively rare, especially in the drier regions of the aridity gradient which are one of our main targets. As aridity increases, the role of water as a limiting factor increases proportionally over the importance of other physical factors such as soil nutrients. This is the basis of convergence to a common RUE across biomes in dry seasons (Huxman et al., 2004), and becomes relevant at the spatial and temporal scales at which this study was done.

The interpretations above used natural or semi-natural vegetation as much as possible, because it represents rather stable and predictable responses to the effects of the drivers used. Proper agricultural land uses show mixed affinities and avoidances across the full spectrum of land condition categories, and do not allow patterns as regular as those commented above to be found. This is the case of non-irrigated arable land, for example, as it contains a broad variety of crops under many management practices. We believe that such moderate dispersion is in fact a subject for the approach reported in this work, rather than an element for interpretation.

6. Conclusion

The approach for the assessment and monitoring of land condition described in this article has demonstrated consistent performance in its application to the Iberian Peninsula. The use of a long period for developing parallel procedures of synchronic assessment and diachronic monitoring was a milestone in overcoming the paradox of monitoring as a sequence of assessments. This is intrinsically contradictory when dealing with complex landscape mosaics, as assessments commonly require relative estimators, the results of which are often difficult to set in a meaningful time sequence. We have based the whole approach on an estimator of vegetation density (GVF) derived from Earth Observation. A relative ratio (rRUE) was used to generate assessment classes, which enabled detrended comparisons across space. However, rates of change in raw GVF over time and aridity were used to generate subclasses of monitoring in terms of trends with respect to those drivers. We believe that, beyond the particular methods used for every procedure, this concept is general and may be applied whenever assessment and monitoring must be performed jointly to detect land condition.

The concrete methodologies developed here for the assessment and monitoring procedures have succeeded in confronting some important challenges. In the first, boundary functions were effective in two ways, statistical detection of reference areas, which is probably a better alternative than their designation by expert, but subjective criteria, and comparable ranges for the calculation of relative RUE across different climate zones. Making the RUE of any given location relative to its most probable range means that locations can be directly compared. As a corollary, different land covers or uses can also be directly compared on that basis, a common limitation in assessment procedures. This was further reinforced by the two time scales used for the computation of mean and extreme RUE, which were useful for improved discrimination of landscape types. With respect to the monitoring procedure, the use of a stepwise multiple regression was demonstrated to be effective in discriminating effects of a drifting climate from other internal trends in vegetation, which can then be attributed to internal dynamics or to land management. Nonetheless, an advantage of this assessment and monitoring approach is the use of a relatively modest input dataset including time-series of an indicator of vegetation density and climate data. Whilst this is not yet readily available for many areas, generic databases are evolving quickly and this or similar models will see increased applications in the near future.

Our approach is not free of problems, however. First of all, it is strictly empirical. Whilst every effort has been made to make vegetation condition values consistent within a given study area and period, there is no explicit link made between statistical procedures and underlying

ecological functions. The boundary functions are selected by best fit, and their shape remains largely unexplained in terms of plant ecophysiology. As a result, absolute references of vegetation performance are lacking in this model and land condition must be assessed by its relative position in an interval. The same is true for the length of the period. So far the only condition is that it should be long enough to account for representative mean and extreme RUE in all locations, and to detect any trend in vegetation density. However, a theoretical framework for the dependency of vegetation growth on climate variability would considerably improve this requirement.

The above limitations are explained in terms of the approach described, but in general terms they are shared by many empirical approaches. The main problem is that existing functional models are difficult if not impossible to parameterise for practical purposes, such as land degradation surveillance. Therefore, for the time being, at least, we will have to live with empirical models. We foresee that in some immediate respects, our model may require attention. The use of a significant number of time lags for extreme RUE instead of a fixed interval of six months would surely enhance its discriminatory capacity. And the representativeness of the study period could possibly be approached by a GVF frequency analysis.

Because of their relevance, two aspects of the methodology reported should be emphasized. First, it should be considered as a language rather than as a self-contained model with fixed steps. The whole is more important here than its individual parts, which may be replaced or upgraded depending on the intended application. For example, detrending observed RUE from aridity is more important than the use of the mean instead of summatory values of the selected vegetation index as an approach to the NPP. Another aspect that could easily be adapted is the specification of assessment categories. For example, lack of knowledge of the study area might make it advisable to use the within-range combination as a relative reference, and call it simply 'normal' rather than 'good condition' as we have done. And second, the nature of the data is more important than any concrete data product. For example, MEDOKADS-GVF was used for this application for the reasons explained in Section 2, but GIMMS-NDVI might be used for a different area if it were considered appropriate. The important point here is that consistent and reliable archived time-series are used according to the general requirements formulated in Section 2.

The Iberian Peninsula was a challenging area to use as a benchmark. As described in the data section, it is a large and complex territory with many sources of land condition variation that operate in many cases at a finer spatial resolution than the one used here. Nevertheless, the model succeeded in detecting interpretable patterns. In very general terms, it shows land to be healthier than expected, with focalised spots of ongoing degradation associated with current or recent intensive land use. Static or positive vegetation growth rates were detected almost everywhere, including Mediterranean areas that were undergoing increased aridification during the study period. The model would therefore depict a landscape matrix in which natural vegetation and areas of inherited desertification are interwoven in a mosaic of static, resilient or thriving patches. Comparatively smaller areas of intense economic development embedded in it would appear, grow, over-grow and decay at a much faster pace than their surrounding landscape. Perhaps the most striking fact detected in this work was that degrading or static trends prevail in degraded or unusually degraded land, whilst trends to improve are represented most in land in good or unusually good condition. This suggests an irreversible divergency in landscape evolution that supports the perceived drama of desertification and is a warning not to overlook degradation hot spots. This will no doubt be a priority target for future work.

Acknowledgements

The authors would like to thank Mr. Leopoldo Rojo, Coordinator of the Spanish National Action Plan to Combat Desertification, and Mr.

Lucio do Rosario, Portuguese Focal Point for the UNCCD, for their valuable insights on the use and interpretation of the research presented in this work. Mr. Rafael Hidalgo, of the Directorate General for Nature Conservation of the Spanish Ministry of Environment and Rural and Marine Affairs, kindly supplied the Natura 2000 network database for Spain and helped us with its interpretation. Three anonymous reviewers made constructive comments and suggestions that improved the manuscript. This research was funded by the European Commission projects LADAMER (ref. EVK2-2002-0599) and DeSurvey (Integrated Project contract No. 003950).

References

- Adeel, Z., Safriel, U., Niemeijer, D., White, R., Kalbermatten, G., Glantz, M., et al. (2005). Millennium Ecosystem Assessment. Ecosystems and Human Well-being: Desertification Synthesis. Washington D.C: World Resources Institute (<http://www.millenniumassessment.org/documents/document.355.aspx.pdf> (Accessed January 2010)).
- Bai, Z. G., Dent, D. L., & Schaepman, M. E. (2005). *Quantitative Global Assessment of Land Degradation and Improvement: pilot study in North China. Report 2005/06*. Wageningen: ISRIC - World Soil Information (<http://www.isric.org/isric/webdocs/Docs/GLADChinaPilot.pdf> (Accessed January 2010)).
- Billing, H. (2007). *Land surface temperature corrected for orbital shift for evaluation test sites (DeSurvey deliverable D 1.5.1.14)*. Berlin: Institut für Meteorologie, Freie Universität (http://wekuw.met.fu-berlin.de/~HeinerBilling/korr_temp/korr_temp.html (Accessed January 2010)).
- Boer, M. M., & Puigdefabregas, J. (2003). Predicting potential vegetation index values as a reference for the assessment and monitoring of dryland condition. *International Journal of Remote Sensing*, 24, 1135–1141.
- Choudhury, B. J. (1989). Estimating evaporation and carbon assimilation using infrared temperature data: vistas in modelling. In G. Asrar (Ed.), *Theory and Applications of Optical Remote Sensing* (pp. 628–690). New York: Wiley and sons.
- Chuvieco, E., Cocero, D., Riaño, D., Marin, P., Martínez-Vega, J., de la Riva, J., & Perez, F. (2004). Combining NDVI and surface temperature for the estimation of live fuel moisture content in forest fire danger rating. *Remote Sensing of Environment*, 92, 322–331.
- Coll, C., & Caselles, V. (1997). A split-window algorithm for land surface temperature from advanced very high resolution radiometer data: Validation and algorithm comparison. *Journal of Geophysical Research*, 102, 16697–16713.
- Coll, C., Caselles, V., Sobrino, J. A., & Valor, E. (1994). On the atmospheric dependence of the split-window equation for land surface temperature. *International Journal of Remote Sensing*, 15, 105–122.
- de Luis, M., Gonzalez-Hidalgo, J. C., Longares, L. A., & Stepanek, P. (2008). Seasonal precipitation trends in the Mediterranean Iberian Peninsula in second half of 20th century. *International Journal of Climatology*, 29, 1312–1323.
- EEC (1992). *Council Directive 92/43/EEC of 21 May 1992 on the conservation of natural habitats and of wild fauna and flora. OJ L206*. : Council of the European Communities (<http://eur-lex.europa.eu/LexUriServ/LexUriServ.do?uri=CONSLEG:1992L0043:20070101:EN:PDF> (Accessed January 2010)).
- EEA (2007). Corine land cover 2000 (CLC2000) seamless vector database. Copenhagen: European Environment Agency (<http://www.eea.europa.eu/data-and-maps/data/corine-land-cover-2000-clc2000-seamless-vector-database> (Accessed January 2010)).
- EROS (1996). Global 30 Arc-Second Elevation Dataset (GTOPO30). US Geological Survey. Sioux Falls: Center for Earth Resources Observation and Science (http://eros.usgs.gov/#/Find_Data/Products_and_Data_Available/GTOPO30 (Accessed January 2010)).
- Friedrich, K., & Koslowsky, D. (2009). Inter-comparison of MEDOKADS and NOAA/NASA pathfinder AVHRR land NDVI time series. In A. Röder, & J. Hill (Eds.), *Recent Advances in Remote Sensing and Geoinformation Processing for Land Degradation Assessment* (pp. 103–116). London: Taylor and Francis.
- Garbulsky, M. F., & Paruelo, J. M. (2004). Remote sensing of protected areas to derive baseline vegetation functioning characteristics. *Journal of Vegetation Science*, 15, 711–720.
- Geerken, R., & Ilaoui, M. (2004). Assessment of rangeland degradation and development of a strategy for rehabilitation. *Remote Sensing of Environment*, 90, 490–504.
- Glickman, T. (Ed.). (2000). *Glossary of Meteorology*. Boston: American Meteorological Society.
- Goetz, S. J., Fiske, G. J., & Bunn, A. G. (2006). Using satellite time-series data sets to analyze fire disturbance and forest recovery across Canada. *Remote Sensing of Environment*, 101, 352–365.
- Gonzalez-Hidalgo, J. C., de Luis, M., Raventos, J., & Sanchez, J. R. (2001). Spatial distribution of seasonal rainfall trends in a western Mediterranean area. *International Journal of Climatology*, 21, 843–860.
- Gonzalez-Hidalgo, J. C., Lopez-Bustins, J. A., Stepanek, P., Martin-Vide, J., & de Luis, M. (2008). Monthly precipitation trends on the Mediterranean fringe of the Iberian Peninsula during the second-half of the twentieth century (1951–2000). *International Journal of Climatology*, 29, 1415–1429.
- Goward, S. N., & Hope, A. S. (1989). Evapotranspiration from combined reflected solar and emitted terrestrial radiation: Preliminary FIFE results from AVHRR data. *Advances in Space Research*, 9, 239–249.

- Guevara, J. C., Estevez, O. R., & Torres, E. R. (1996). Utilization of the rain-use efficiency factor for determining potential cattle production in the Mendoza plain, Argentina. *Journal of Arid Environments*, 33, 347–353.
- Hargreaves, G. H., & Samani, Z. A. (1982). Estimating potential evapotranspiration. *Journal of the Irrigation & Drainage Division - ASCE*, 108, 225–230.
- Hein, L., & de Ridder, N. (2006). Desertification in the Sahel: A reinterpretation. *Global Change Biology*, 12, 751–758.
- Hellden, U., & Tottrup, C. (2008). Regional desertification: A global synthesis. *Global and Planetary Change*, 64, 169–176.
- Herrmann, S. M., Anyamba, A., & Tucker, C. J. (2005). Recent trends in vegetation dynamics in the African Sahel and their relationship to climate. *Global Environmental Change-Human and Policy Dimensions*, 15, 394–404.
- Hielkema, J. U., Prince, S. D., & Astle, W. L. (1987). Monitoring of global vegetation dynamics for assessment of primary productivity using NOAA advanced very high resolution radiometer. *Advances in Space Research*, 7, 81–88.
- Hill, J., Stellmes, M., Udelhoven, T., Roder, A., & Sommer, S. (2008). Mediterranean desertification and land degradation Mapping related land use change syndromes based on satellite observations. *Global and Planetary Change*, 64, 146–157.
- Holben, B. N. (1986). Characterization of maximum value composites from temporal AVHRR data. *International Journal of Remote Sensing*, 7, 1417–1434.
- Hutchinson, M. F. (1995). Interpolating mean rainfall using thin-plate smoothing splines. *International Journal of Geographical Information Systems*, 9, 385–403.
- Hutchinson, M. F., & Gessler, P. E. (1994). Splines – More than just a smooth interpolator. *Geoderma*, 62, 45–67.
- Huxman, T. E., Smith, M. D., Fay, P. A., Knapp, A. K., Shaw, M. R., Loik, M. E., et al. (2004). Convergence across biomes to a common rain-use efficiency. *Nature*, 429, 651–654.
- Jarvis, C. H., & Stuart, N. (2001). A comparison among strategies of interpolating maximum and minimum daily air temperatures. Part I: The selection of “guiding” topographic and land cover variables. *Journal of Applied Meteorology*, 40, 1060–1074.
- Koslowsky, D. (1996). *Mehrjährige validierte und homogenisierte Reihen des Reflexionsgrades und des Vegetationsindexes von Landoberflächen aus täglichen AVHRR-Daten hoher Auflösung*. Berlin: Institute for Meteorology, Free University Berlin.
- Koslowsky, D. (1998). Daily extended 1-km AVHRR data sets of the Mediterranean. *9th Conf. Sat. Meteor. and Oceanogr.* (pp. 38–41). Paris: UNESCO.
- LADA (2006). Land Degradation Assessment in Drylands. Rome: LADA Secretariat, FAO (<http://www.fao.org/nr/lada/>) (Accessed January 2010).
- Lambin, E. F., & Ehrlich, D. (1996). The surface temperature-vegetation index space for land cover and land-cover change analysis. *International Journal of Remote Sensing*, 17, 463–487.
- Lambin, E. F., & Ehrlich, D. (1997). Land-cover changes in sub-Saharan Africa (1982–1991): application of a change index based on remotely sensed surface temperature and vegetation indices at a continental scale. *Remote Sensing of Environment*, 61, 181–200.
- Lasanta, T., & Vicente-Serrano, S. M. (2006). Factores en la variabilidad espacial de los cambios de cubierta vegetal en el Pirineo. *Cuadernos de Investigación Geográfica*, 32, 57–80.
- LeHouerou, H. N. (1984). Rain Use Efficiency – A unifying concept in arid-land ecology. *Journal of Arid Environments*, 7, 213–247.
- MARM (2006). The Natura 2000 network in Spain. Madrid: Ministerio de Medio Ambiente y Medio Rural y Marino (<http://www.mma.es/portal/secciones/biodiversidad/rednatura2000/>) (Accessed January 2010).
- McKenney, D. W., Pedlar, J. H., Papadopol, P., & Hutchinson, M. F. (2006). The development of 1901–2000 historical monthly climate models for Canada and the United States. *Agricultural and Forest Meteorology*, 138, 69–81.
- Mulligan, M., Burke, S. M., & Ramos, M. C. (2004). Climate change, land-use change and the “desertification” of Mediterranean Europe. In S. Mazzoleni, G. di Pasquale, M. Mulligan, P. di Martino, & F. Rego (Eds.), *Recent Dynamics of the Mediterranean Vegetation and Landscape* (pp. 259–279). Chichester: John Wiley & Sons Ltd.
- Myneni, R. B., Keeling, C. D., Tucker, C. J., Asrar, G., & Nemani, R. R. (1997). Increased plant growth in the northern high latitudes from 1981 to 1991. *Nature*, 386, 698–702.
- Nemani, R., Pierce, L., Running, S. W., & Goward, S. (1993). Developing satellite derived estimates of surface moisture status. *Journal of Applied Meteorology*, 32, 548–557.
- Oldeman, L. R., Hakkeling, R. T. A., & Sombroek, W. G. (1991). World map of the status of human-induced soil degradation: an explanatory note. *Global Assessment of Soil Degradation (GLASOD)*. Wageningen: International Soil Reference and Information Centre / UNEP (<http://www.isric.org/UK/About+ISRIC/Projects/Track+Record/GLASOD.htm>) (Accessed January 2010).
- Olsson, L., Eklundh, L., & Ardö, J. (2005). A recent greening of the Sahel – Trends, patterns and potential causes. *Journal of Arid Environments*, 63, 556–566.
- Pickup, G. (1996). Estimating the effects of land degradation and rainfall variation on productivity in rangelands: An approach using remote sensing and models of grazing and herbage dynamics. *Journal of Applied Ecology*, 33, 819–832.
- Pickup, G., Bastin, G. N., & Chewings, V. H. (1994). Remote-sensing-based condition assessment for nonequilibrium rangelands under large-scale commercial grazing. *Ecological Applications*, 4, 497–517.
- Price, J. C. (1993). Estimating leaf area index from satellite data. *IEEE Transactions on Geoscience and Remote Sensing*, 31, 727–734.
- Price, D. T., McKenney, D. W., Nalder, I. A., Hutchinson, M. F., & Kesteven, J. L. (2000). A comparison of two statistical methods for spatial interpolation of Canadian monthly mean climate data. *Agricultural and Forest Meteorology*, 101, 81–94.
- Prince, S. D., De Colstoun, E. B., & Kravitz, L. L. (1998). Evidence from rain-use efficiencies does not indicate extensive Sahelian desertification. *Global Change Biology*, 4, 359–374.
- Prince, S. D., Wessels, K. J., Tucker, C. J., & Nicholson, S. E. (2007). Desertification in the Sahel: A reinterpretation of a reinterpretation. *Global Change Biology*, 13, 1308–1313.
- Puigdefabregas, J., & Mendizabal, T. (1998). Perspectives on desertification: Western Mediterranean. *Journal of Arid Environments*, 39, 209–224.
- Sandholt, I., Rasmussen, K., & Andersen, J. (2002). A simple interpretation of the surface temperature/vegetation index space for assessment of surface moisture status. *Remote Sensing of Environment*, 79, 213–224.
- Siegel, S., & Castellan, N. J. (1988). *Nonparametric Statistics for the Behavioural Sciences*. Boston: McGraw-Hill.
- Soanes, C., & Stevenson, A. (2005). *Oxford Dictionary of English*. Oxford: Oxford University Press.
- Sokal, R. R., & Rohlf, F. J. (1995). *Biometry*. New York: W.H. Freeman and Co.
- Stellmes, M., Sommer, S., & Hill, J. (2005). Use of the NOAA AVHRR NDVI-Ts feature space to derive vegetation cover estimates from long term time series for determining regional vegetation trends in the Mediterranean. In A. Röder & J. Hill (Eds.), *Proceedings of the 1st International Conference on Remote Sensing and Geoinformation Processing in the Assessment and Monitoring of Land Degradation and Desertification* (pp. 231–238). Trier: University of Trier (<http://ubt.opus.hbz-nrw.de/volltexte/2006/362/>) (Accessed April 2010).
- Tucker, C. J. (1979). Red and photographic infrared linear combinations for monitoring vegetation. *Remote Sensing of Environment*, 8, 127–150.
- Tucker, C. J., Justice, C. O., & Prince, S. D. (1986). Monitoring the grasslands of the Sahel 1984–1985. *International Journal of Remote Sensing*, 7, 1571–1581.
- Tucker, C. J., & Nicholson, S. E. (1999). Variations in the size of the Sahara Desert from 1980 to 1997. *Ambio*, 28, 587–591.
- Udelhoven, T., Stellmes, M., del Barrio, G., & Hill, J. (2009). Assessment of rainfall and NDVI anomalies in Spain (1989–1999) using distributed lag models. *International Journal of Remote Sensing*, 30, 1961–1976.
- UNEP (1992). *World Atlas of Desertification*. Nairobi: UNEP.
- Veron, S. R., Paruelo, J. M., & Oesterheld, M. (2006). Assessing desertification. *Journal of Arid Environments*, 66, 751–763.
- Vicente-Serrano, S. M., Cuadrat-Prats, J. M., & Romo, A. (2006). Aridity influence on vegetation patterns in the middle Ebro Valley (Spain): Evaluation by means of AVHRR images and climate interpolation techniques. *Journal of Arid Environments*, 66, 353–375.
- Vicente-Serrano, S. M., Lasanta, T., & Romo, A. (2003). Diferencias espaciales en la evolución del NDVI en la cuenca alta del Aragón: Efectos de los cambios en el uso del suelo. *Cuadernos de Investigación Geográfica*, 29, 51–66.
- Vicente-Serrano, S. M., Lasanta, T., & Romo, A. (2004). Analysis of spatial and temporal evolution of vegetation cover in the Spanish central pyrenees: Role of human management. *Environmental Management*, 34, 802–818.
- Weissteiner, C. J., Böttcher, K., Mehl, W., Sommer, S., & Stellmes, M. (2008). Mediterranean-wide Green Vegetation Abundance for Land Degradation Assessment Derived from AVHRR NDVI and Surface Temperature 1989 to 2005. Luxembourg: European Commission - JRC (http://desert.jrc.ec.europa.eu/action/documents/CWeissteiner_GVF2008.pdf) (Accessed January 2010).
- Wessels, K. J., Prince, S. D., Malherbe, J., Small, J., Frost, P. E., & VanZyl, D. (2007). Can human-induced land degradation be distinguished from the effects of rainfall variability? A case study in South Africa. *Journal of Arid Environments*, 68, 271–297.
- Wessels, K. J., Prince, S. D., & Reshef, I. (2008). Mapping land degradation by comparison of vegetation production to spatially derived estimates of potential production. *Journal of Arid Environments*, 72, 1940–1949.
- Yan, H., Nix, H. A., Hutchinson, M. F., & Booth, T. H. (2005). Spatial interpolation of monthly mean climate data for China. *International Journal of Climatology*, 25, 1369–1379.